A single cytochrome P450 oxidase from Solanum habrochaites sequentially oxidizes 7-epi-zingiberene to derivatives toxic to whiteflies and various microorganisms

Zabel, S.; Brandt, W.; Porzel, A.; Athmer, B.; Bennewitz, S.; Schäfer, P.; Kortbeek, R.; Bleeker, P.; Tissier, A.

DOI
10.1111/tpj.15113

Publication date
2021

Document Version
Final published version

Published in
Plant Journal

the plant journal

SEB SOCIETY FOR EXPERIMENTAL BIOLOGY

The Plant Journal (2021) **105,** 1309–1325 doi: 10.1111/tpj.15113

A single cytochrome P450 oxidase from *Solanum habrochaites* sequentially oxidizes 7-*epi*-zingiberene to derivatives toxic to whiteflies and various microorganisms

Sebastian Zabel[1,4], Wolfgang Brandt[2], Andrea Porzel[2], Benedikt Athmer[1], Stefan Bennewitz[1], Petra Schäfer[1], Ruy Kortbeek[3], Petra Bleeker[3] and Alain Tissier[1,5,*]

[1]*Department of Cell and Metabolic Biology, Leibniz-Institute of Plant Biochemistry, Weinberg 3, Halle 06120, Germany,*
[2]*Department of Bioorganic Chemistry, Leibniz-Institute of Plant Biochemistry, Weinberg 3, Halle 06120, Germany,*
[3]*Swammerdam Institute for Life Sciences, Green Life Sciences Research Cluster, University of Amsterdam, Science Park 904, Amsterdam 1098 XH, The Netherlands,*
[4]*IDT Biologika Deutschland, Am Pharmapark, Dessau-Rosslau 06861, Germany, and*
[5]*VERROVACCiNES GmbH, Blücherstraße 26, Halle (Saale) 06120, Germany*

Received 22 July 2020; revised 30 October 2020; accepted 30 November 2020; published online 4 December 2020.
*For correspondence (e-mail alain.tissier@ipb-halle.de)

SUMMARY

Secretions from glandular trichomes potentially protect plants against a variety of aggressors. In the tomato clade of the *Solanum* genus, glandular trichomes of wild species produce a rich source of chemical diversity at the leaf surface. Previously, 7-*epi*-zingiberene produced in several accessions of *Solanum habrochaites* was found to confer resistance to whiteflies (*Bemisia tabaci*) and other insect pests. Here, we report the identification and characterisation of 9-hydroxy-zingiberene (9HZ) and 9-hydroxy-10,11-epoxyzingiberene (9H10epoZ), two derivatives of 7-*epi*-zingiberene produced in glandular trichomes of *S. habrochaites* LA2167. Using a combination of transcriptomics and genetics, we identified a gene coding for a cytochrome P450 oxygenase, ShCYP71D184, that is highly expressed in trichomes and co-segregates with the presence of the zingiberene derivatives. Transient expression assays in *Nicotiana benthamiana* showed that ShCYP71D184 carries out two successive oxidations to generate 9HZ and 9H10epoZ. Bioactivity assays showed that 9-hydroxy-10,11-epoxyzingiberene in particular exhibits substantial toxicity against *B. tabaci* and various microorganisms including *Phytophthora infestans* and *Botrytis cinerea*. Our work shows that trichome secretions from wild tomato species can provide protection against a wide variety of organisms. In addition, the availability of the genes encoding the enzymes for the pathway of 7-*epi*-zingiberene derivatives makes it possible to introduce this trait in cultivated tomato by precision breeding.

Keywords: *Solanum habrochaites*, cytochrome P450, glandular trichomes, specialized metabolism, 7-*epi*-zingiberene, *Bemisia tabaci*, *Phytophthora infestans*, *Botrytis cinerea*.

INTRODUCTION

The plant surface constitutes the first barrier against various aggressors, including pathogens and herbivores. In the aerial parts, different types of protuberances can differentiate and contribute to the protection of plants. The most prominent of these are trichomes, which are uni- or multicellular structures derived from the epidermis that can be either glandular or non-secreting. Glandular trichomes typically contain one to several highly metabolically active cells dedicated to the production of large quantities of specialized metabolites (Tissier, 2012; Schurink and Tissier, 2020). The compounds produced can be stored in a specialized cavity, which is typical for volatiles (e.g. mono- and sesquiterpenes), or secreted onto the leaf surface, as in the case of the resinous acyl sugars or diterpenoids in several Solanaceae species (Choi *et al.*, 2012; Tissier *et al.*, 2017). In the tomato genus, including both cultivated and related wild species, different types of glandular trichomes specialized in the production of distinct classes of substances can be found (Luckwill, 1943). Type I and IV trichomes typically produce acyl sugars that are directly secreted from the tip of the glandular cells (King *et al.*, 1990; Schilmiller *et al.*, 2012). Type VI glandular trichomes constitute one of the most abundant types, and in cultivated tomato, *Solanum lycopersicum*, their main

products are monoterpenes (Schilmiller *et al.*, 2009). Whereas little, if any, variation in the composition of the type VI secretions has been reported within *S. lycopersicum* accessions, related species, in particular *Solanum habrochaites*, display an impressive diversity of chemotypes (Coates *et al.*, 1988; Snyder *et al.*, 1993; Breeden and Coates, 1994; Gonzales-Vigil *et al.*, 2012). Except in some accessions of *S. habrochaites* ssp. *glabratum*, where the main compounds produced are the fatty acid-derived methyl ketones (Farrar and Kennedy, 1987; Fridman *et al.*, 2005), mono- and sesquiterpenoids are the dominant products in type VI trichomes.

Two main classes of sesquiterpenoids have been described in tomato (van Der Hoeven *et al.*, 2000). Class I sesquiterpenoids are synthesized from the cytosolic *trans,-trans*-farnesyl diphosphate (FDP) (*E,E*-FDP) and consist of a mixture of various germacrene sesquiterpenes as well as farnesoic and/or dehydro-farnesoic acids in some accessions (Snyder *et al.*, 1993; Breeden *et al.*, 1996; van Der Hoeven *et al.*, 2000). Class II sesquiterpenes are derived from *cis,cis*-FDP (*Z,Z*-FDP) by plastid-localized *cis,cis*-farnesyl diphosphate synthase (zFPS) in *S. habrochaites* accessions exclusively (Sallaud *et al.*, 2009). Until now two sesquiterpene synthases able to convert *Z,Z*-FDP have been identified in *S. habrochaites*. Santalene and bergamotene synthase (ShSBS) is a multiproduct cyclase which makes (+)-α-santalene, (+)-*endo*-β-bergamotene and (−)-*endo*-β-bergamotene as well as other minor products (Sallaud *et al.*, 2009). The other sesquiterpene cyclase (ShZIS) synthesizes 7-*epi*-zingiberene (hereafter 7*epi*Z; Figure 1, peak 1) as the main product, which can spontaneously oxidize to *R*-curcumene (Bleeker *et al.*, 2012; Gonzales-Vigil *et al.*, 2012). Accessions that make santalene and bergamotene do not produce 7*epi*Z, and vice versa, indicating that the corresponding enzymes are encoded by different alleles of the same gene (Gonzales-Vigil *et al.*, 2012). The santalene and bergamotene sesquiterpenes are further oxidized to carboxylic acids, which are, in some accessions such as LA1777, by far the most abundant compounds produced in type VI trichomes, in amounts that can reach tens of milligrams per leaf fresh weight (Frelichowski and Juvik, 2005). For all these compounds, activities towards various insect herbivores has been demonstrated. For example, the sesquiterpene carboxylic acids from LA1777 were shown to confer resistance against two lepidopteran pests, *Helicoverpa zea* and *Spodoptera exigua* (Frelichowski and Juvik, 2001). Also, 7*epi*Z, produced in trichomes of *S. habrochaites* accessions PI127826 and LA2167, amongst others, seems to confer a particularly broad range of resistance against various pests. These include pinworms (*Tuta absoluta*), whiteflies (*Bemisia tabaci*), spider mite (*Tetranychus evansi*) and Colorado potato beetle (*Leptinotarsa decemlineata*) (Carter *et al.*, 1989; Maluf *et al.*, 2001, 2010; Freitas *et al.*, 2002; de Azevedo *et al.*, 2003; Goncalves *et al.*, 2006). Moreover, transformation of cultivated tomato with the two genes required for the biosynthesis of 7*epi*Z (i.e. *zFPS* and *ShZIS*) also resulted in improved insect resistance due to increased repellence of whiteflies and toxicity to spider mites (Bleeker *et al.*, 2012).

While surveying the exudate profiles of various accessions of *S. habrochaites*, we noted the presence of additional peaks in accession LA2167 that, based on their mass fragmentation pattern, were suggested to be derivatives of 7*epi*Z. Using a combination of mass spectrometry, nuclear magnetic resonance (NMR) spectroscopy, circular dichroism and substrate docking studies, the derivatives were identified as (4*R*,7*R*,9*S*)-7-*epi*-9-hydoxy-zingiberene and (4*R*,7*R*,9*S*,10*S*)-7-*epi*-9-hydroxy-10,11-epoxy-zingiberene. Furthermore, using genetic and transcriptomics approaches we identified a single gene, encoding a cytochrome P450 oxygenase, responsible for their biosynthesis as demonstrated by *in planta* assays. Finally, bioassays with whiteflies (*B. tabaci*) and several microorganisms showed that 9-hydroxy-7-zingiberene (9HZ) and 9-hydroxy-10,11-epoxyzingiberene (9H10epoZ), rather than 7*epi*Z, are responsible for the biological activity, supporting their role in the defence of tomato plants against various pests.

RESULTS

Identification and structure elucidation of two 7-*epi*-zingiberene derivatives

A metabolic profiling survey of different accessions of the wild tomato *S. habrochaites* revealed that, besides 7*epi*Z, two unknown major peaks are present in leaf surface extracts of LA2167 measured by gas chromatography-mass spectrometry (GC-MS) (Figure 1). The mass spectra of these compounds did not yield any convincing match in the NIST database, indicating that these might be as yet uncharacterized compounds. However, the spectra did present significant similarities to that of 7*epi*Z (compound 1, molecular mass 204), suggesting they might be derivatives thereof, with a molecular mass of 220 for compound 2 and 236 for compound 3 (Figure 1). This increase in molecular mass corresponds to one and two oxygen atoms for compounds 2 and 3, respectively, and is consistent with increased retention times upon GC. To characterize these compounds further, leaf surface extracts were derivatized by silylation and analysed by GC-MS. This analysis showed that compound 2 contains one hydroxyl group and compound 3 one hydroxyl group plus one oxygen atom that cannot be derivatized, which could for example indicate the presence of an epoxide (for details see Figures S1–S3 in the online Supporting Information).

Next, we purified compounds 2 and 3 from *S. habrochaites* LA2167 leaf surface extracts (see Experimental Procedures and Figure S4). After purification, 21 mg of compound 2 and 25 mg of compound 3 were recovered.

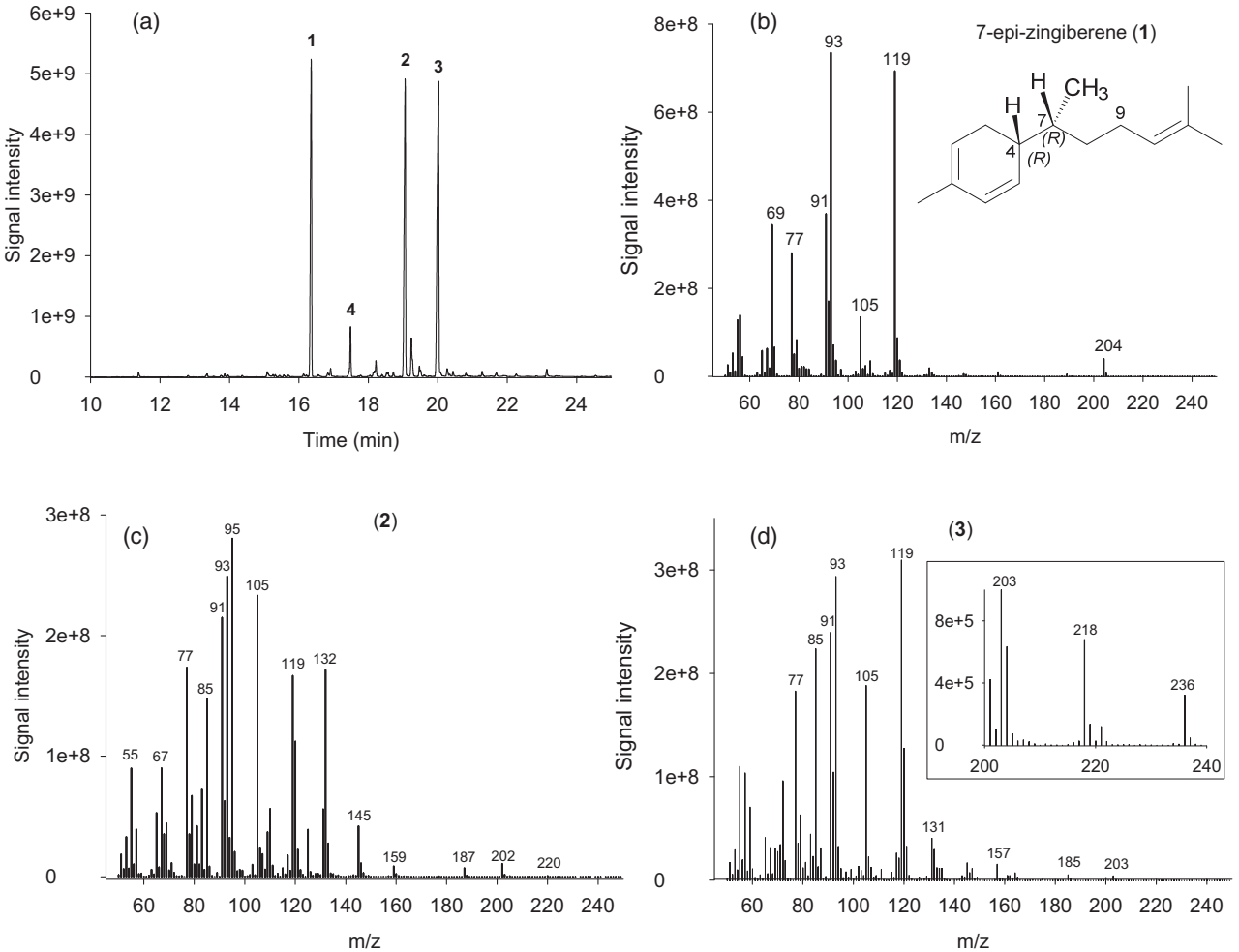

Figure 1. Gas chromatography mass spectrometry (GC-MS) analysis of leaf surface extracts of *Solanum habrochaites* LA2167.
(a) A GC-MS total ion count chromatogram (TIC) of a leaf surface hexane extract of *S. habrochaites* LA2167. Peak 1 is 7-*epi*-zingiberene, peaks 2 and 3 are zingiberene derivatives that are characterized in this work and peak 4 is germacrene B.
(b) Mass spectrum of 7-*epi*-zingiberene.
(c) Mass spectrum of compound 2.
(d) Mass spectrum of compound 3. The insert is a zoomed-in section between *m/z* 200 and 240.

Compounds 2 and 3 were then analysed by electrospray high resolution mass spectrometry (ESI-HRMS) in positive mode giving monoisotopic molecular masses of 221.1900 and 237.1849, respectively, confirming the predicted formula $C_{15}H_{24}O$ for compound 2 and $C_{15}H_{24}O_2$ for compound 3 (Figures S5 and S6).

The structures of compounds 2 and 3 were elucidated on the basis of extensive one-dimensional (1D) (^{1}H, ^{13}C) and 2D (COSY, HSQC, HMBC) nuclear magnetic resonance NMR spectroscopic analysis. Detailed analysis of ^{1}H,^{1}H COSY and ^{1}H,^{13}C HMBC 2D spectra (Figure S7 and Table 1) and comparison with literature data (Ishii *et al.*, 2011) revealed compound 2 to be 9HZ (Figure 2). Similarly, based on analysis of ^{1}H,^{1}H COSY and ^{1}H,^{13}C HMBC 2D spectra (Table 2), the structure of compound 3 was established as 9H10epoZ (Figure 2). Notably, the NMR data were not sufficient to determine the absolute configuration of 9HZ and 9H10epoZ. 9-Hydroxy-zingiberene and 9H10epoZ have three and four chiral centres, respectively. Since they are derived from 7*epi*Z, whose absolute configuration has been determined to be 4*R*,7*R*, there are two and four possible stereoisomers for 9HZ and 9H10epoZ, respectively. Because biological activity is often associated with specific stereoisomers, we sought to determine the absolute configuration of the tomato zingiberene derivatives. In the absence of crystals of these compounds, this issue was addressed using circular dichroism and substrate docking studies, the latter requiring the identification of the enzyme catalysing the oxidation of 7*epi*Z (see below).

Identification of a candidate gene for the biosynthesis of the 7-*epi*-zingiberene derivatives

To identify the genes involved in the biosynthesis of 9HZ and 9H10epoZ, we used two complementary approaches,

Table 1 The NMR data for compound 2 (solvent C_6D_6; for the numbering scheme see Figure 2). The ^{13}C and DEPT spectra of compound 2 exhibit signals for four methyl, two methylene and seven methine groups as well as two quaternary carbons. As can be seen from their low-field ^{13}C chemical shifts, the quaternary ($\delta^{13}C$ 133.9, 131.2 p.p.m.) and four of the tertiary carbons ($\delta^{13}C$ 129.8, 129.6, 128.8, 120.9 p.p.m.) belong to double bond units. One of the two remaining methine groups shows a hydroxyl substituent ($\delta^{13}C$ 67.0 p.p.m.; $\delta^{1}H$ 4.356 p.p.m.)

Pos.	$\delta^{13}C$ (p.p.m.)	$\delta^{1}H$ (p.p.m.) *m* [J (Hz)]	HMBC correlation H to C
1	131.2	–	
2	128.8	5.829 ddd (9.7/3.4/1.7)	3, 4, 6
3	129.6	5.684 dd (9.7/3.4)	1, 2, 4, 5, 7
4	38.7	2.377*m*	
5	26.5	2.04[a]	1, 3, 4, 6, 7
6	120.9	5.427*m*	15
7	33.5	1.66[a]	3, 4, 5, 8, 14
8	42.3	1.553 ddd (13.4/7.2/5.2); 1.496 ddd (13.4/8.6/6.7)	4, 7 ,9, 10, 14
9	67.0	4.356 ddd (8.7/7.2/6.7	11
10	129.8	5.110 d sept(8.7/1.4)	12, 13
11	133.9	–	
12	25.7	1.557 d (1.4)	10, 11, 13
13	18.0	1.475 d (1.4)	10, 11, 12
14	17.6	0.910 d (6.8)	4, 7, 8
15	21.2	1.663 br s	1, 2, 6

[a]H chemical shift extracted from the HSQC spectrum.

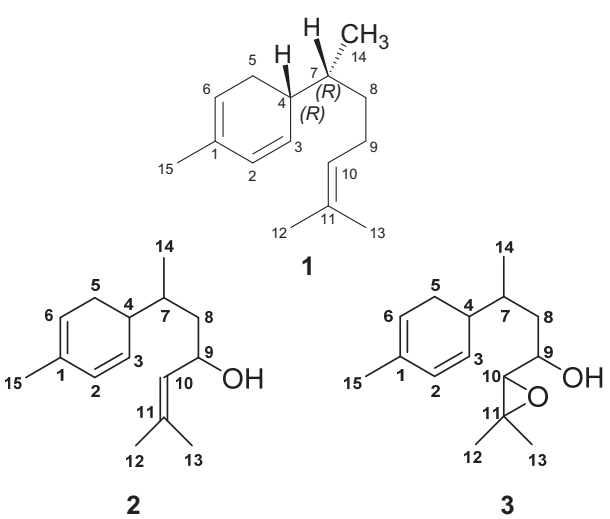

Figure 2. Structure of 7*epi*Z and of compounds 2 and 3 as determined by NMR spectroscopy.
Compounds 2 and 3 were determined to be 9-hydroxy-zingiberene (9HZ) and 9-hydroxy-10,11-epoxy-zingiberene (9H10epoZ), respectively.

transcriptomics and genetics. For transcriptomics, we carried out RNA microarray hybridization with trichome RNA from five *S. habrochaites* accessions that differ in their sesquiterpene composition (Dataset S1). Among these accessions, LA2167 is the only one that produces oxidized

Table 2 The NMR data for compound 3 (solvent C_6D_6; for the numbering scheme see Figure 2). The NMR spectra of compound 3 largely resemble those of 9-hydroxy-zingiberene (9HZ). However, the signals of CH-10 ($\delta^{13}C$ 128.9 p.p.m.; $\delta^{1}H$ 5.110 p.p.m.) and C-11 ($\delta^{13}C$ 133.9 p.p.m.) in 9HZ are replaced in compound 3 by signals at $\delta^{13}C$ 68.1 p.p.m.; $\delta^{1}H$ 2.558 p.p.m. and $\delta^{13}C$ 58.9 p.p.m., respectively. The coupling constant of C-10/H-10 was extracted from the residual ^{1}J correlation peak in the HMBC spectrum. Its size of 170 Hz with a simultaneous high-field shift of H-10 clearly shows CH-10 to be involved in an epoxy unit

Pos.	$\delta^{13}C$ (p.p.m.)	$\delta^{1}H$ (p.p.m.) *m* [J (Hz)]	HMBC correlation H to C
1	131.2	–	
2	129.0	5.822 ddd (9.8/3.4/1.7)	1, 4, 6, 15
3	129.0	5.618 dd (9.8/3.3)	1, 4, 5, 6, 7
4	37.8	2.346 d	3, 9
5	26.6	2.02[a]	1, 3, 4, 6, 7
6	121.0	5.419*m*	4, 5, 15
7	32.9	1.748*m*	4, 5, 8, 9, 14
8	38.4	1.476 ddd (14.0/6.6/5.2); 1.435 ddd (14.0/8.3/7.0)	4, 7 ,9, 10, 14
9	69.0	3.442 ddd (8.3/7.8/5.2)	7, 8, 10, 11
10	68.1	2.558 d (7.8)	8, 9, 11, 12
11	58.9	–	
12[b]	24.8	1.058 s	10, 11, 13
13[b]	19.4	1.046 s	10, 11, 12
14	18.2	0.906 d (6.9)	4, 7, 8
15	21.2	1.663 br s	1, 2, 6

[a]H chemical shift extracted from the HSQC spectrum.
[b]May be interchanged.

zingiberenoids (Figure S8a). We searched for genes annotated as oxidases, particularly cytochrome P450 oxygenases (CYPs) that are overexpressed in LA2167 compared with the other accessions. This resulted in a set of three CYP-encoding genes, of which *Sohab01g008670* (defined by similarity to *Solyc01g008670* of *S. lycopersicum*) showed particularly strong expression in LA2167 (Figure 3a). The expression of this gene was then verified by quantitative RT-PCR, which confirmed the particularly high expression of *Sohab01g008670* in accession LA2167 (Figure 3b). Notably, accessions that produce 7*epi*Z but no oxidized derivatives (LA1753, LA2196, LA2650; Figure S8) have comparatively low expression levels of *Sohab01g008670* (Figure 3b).

In parallel, we generated a backcross population (BC_1F_1) between *S. habrochaites* LA2167 and *S. lycopersicum* LA4024, using LA4024 as the recurrent parent. F_1 plants exhibited an exudate profile that was a combination of that of both parents, including 9HZ and 9H10epoZ, indicating that biosynthesis of the zingiberene derivatives is a dominant trait. Profiling the exudates of 150 BC_1F_1 plants by GC-MS showed a Mendelian segregation for zingiberene and its derivatives (see Table 3). Notably, both zingiberene derivatives strictly co-segregated, indicating that a single locus was responsible for the biosynthesis of these compounds. Furthermore, approximately

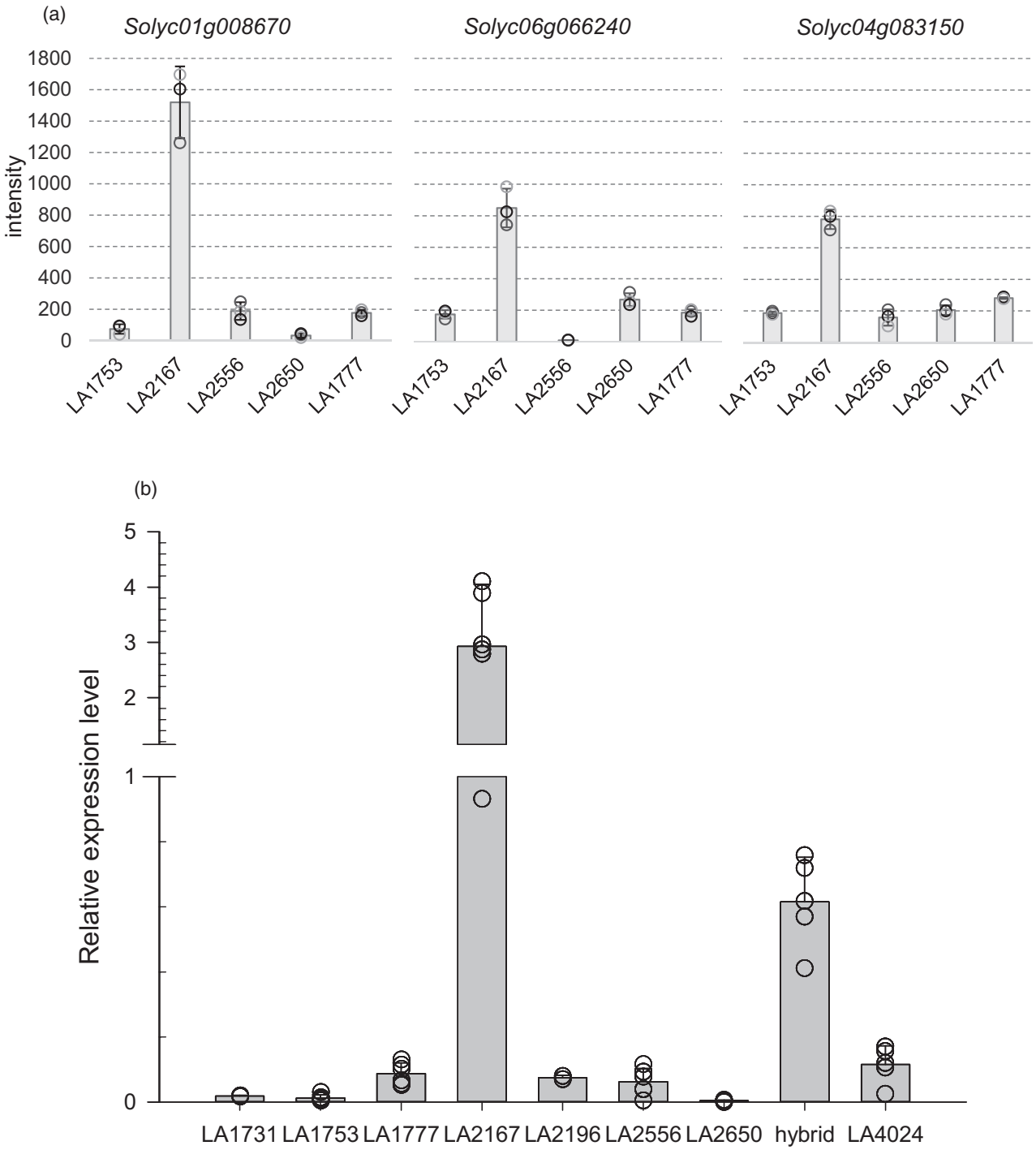

Figure 3. Expression of cytochrome P450 oxygenase (CYP)-encoding candidate genes for the oxidation of zingiberene in various *Solanum habrochaites* accessions.
(a) Microarray data for three CYP-encoding genes in five different accessions. LA2167 is the only accession that produces 7-*epi*-zingiberene and associated derivatives. Intensity designates the normalized fluorescence signal from the microarray.
(b) Quantitative real-time PCR of Sohab01g008670 in different tomato accessions. 'Hybrid' designates F_1 plants of a cross between LA2167 *(S. habrochaites*) and LA4024 (*S. lycopersicum*).

half of the zingiberene-producing lines also produced the zingiberene derivatives, demonstrating that these two loci are not linked. The BC1 population was genotyped using a set of 115 markers distributed over the 12 chromosomes (Dataset S2). Of all markers, only the one corresponding to the *Solyc01g008670*/*Sohab01g008670* locus

showed a strict association with the presence of 9HZ and 9H10epoZ (see Dataset S3 for the full set of data).

Sohab01g008670 and *Solyc01g008670* share 96.6% and 94% identity at the nucleotide level and amino acid level, respectively (Figure S9) and could therefore be considered orthologs. According to the cytochrome P450 oxygenase nomenclature (Nelson, 2009), Sohab01g008670 and Solyc01g008670 were named ShCYP71D184 and SlCYP71D184, respectively. A phylogenetic analysis showed that ShCYP71D184 is closely related to CYP71 enzymes from other Solanaceae species. These include premnaspirodiene oxygenase (CYP71D55) from Egyptian henbane (*Hyoscyamus muticus*) and *epi*-aristolochene 1,3-dihydroxylase (CYP71D20) from tobacco (*Nicotiana tabacum*) (Figure S10). Notably, both CYP71D55 and CYP71D20 carry out successive oxidations of sesquiterpenes (Ralston *et al.*, 2001; Takahashi *et al.*, 2005; Takahashi *et al.*, 2007). These results, together with the mapping and gene expression analysis, provide support for *ShCYP71D184* as a candidate responsible for 7*epi*Z oxidation, warranting further characterization of this protein.

ShCYP71D184 oxidizes 7-*epi*-zingiberene to 9HZ and 9H10epoZ

To evaluate the enzymatic activity of ShCYP71D184, we expressed the full-length coding sequence transiently in *N. benthamiana* leaves together with the enzymes required for the production of 7*epi*Z, namely zFPS and ShZIS from *S. habrochaites* (Sallaud *et al.*, 2009; Bleeker *et al.*, 2012). Surface extracts of agro-infiltrated *N. benthamiana* leaves were analysed by GC-MS 5 days after infiltration. Expression of zFPS alone resulted in the detection of small amounts of *Z,Z*-farnesol, the dephosphorylated form of *Z,Z*-FDP. As expected, expressing zFPS together with ShZIS resulted in the production of 7*epi*Z and small amounts of its aromatized form *R*-curcumene (compounds 1 and 4 in Figure 4a). Co-expression of ShCYP71D184 with zFPS and ShZIS resulted in the production of several additional compounds. Comparison with a leaf surface extract of LA2167 revealed that both 9HZ and 9H10epoZ were present (Figures 4a and S11). There was one additional major peak, whose size varied between repetitions, but which was typically larger than that of 9H10epoZ. This unidentified product is also present in LA2167 leaf surface extracts, although there it is less abundant than 9HZ and 9H10epoZ (compound 6 in Figure 4). The similarity of the mass spectrum of this unidentified compound to that of *R*-curcumene, and its molecular mass of 234 (Figure S11), suggest that it could be 9-hydroxy-10,11-epoxy-curcumene.

Table 3 Segregation of 7-*epi*-zingiberene (7*epi*Z), 9-hydroxy-zingiberene (9HZ) and 9-hydroxy-10,11-epoxyzingiberene (9H10epoZ) in the backcross population. The presence or absence (+ or −) of 7*epi*Z, 9HZ and 9H10epoZ in backcross plants was determined by gas chromatography-mass spectrometry. The observed and expected numbers of plants with a given chemotype are indicated in the two bottom lines (df, degrees of freedom). The probability for the null hypothesis (the expected and observed distributions are identical) is 0.80, supporting the existence of two loci segregating independently

Metabolite	Categories of metabolic profile			Chi-square value (df = 2)/(probability)
7*epi*Z	−	+	+	
9HZ	−	−	+	
9H10epoZ	−	−	+	
No. of plants (n = 150)	73	41	36	0.44 (0.80)
Expected number of plants for two loci	75	37	37	

To demonstrate conclusively that ShCYP71D184 performs the two successive oxidations on 7*epi*Z, we expressed ShCYP71D184 and SlCYP71D184 in yeast and carried out *in vitro* activity assays with purified 7*epi*Z and 9HZ using microsome fractions. ShCYP71D184 was able to produce both 9HZ and 9H10epoZ with 7epiZ as the substrate (Figure 4b). Furthermore, ShCYP71D184 could convert 9HZ to 9H10epoZ (Figure S12). In contrast, no product could be detected with SlCYP71D184, regardless of the substrate used. Together, the results show that ShCYP71D184 is a 7*epi*Z oxidase, henceforth abbreviated as ShZO.

Determination of the absolute configuration of 9HZ and 9H10epoZ

Chiral centres are present at positions 4, 7 and 9 for 9HZ and 4, 7, 9 and 10 for 9H10epoZ. Therefore, the theoretical number of stereoisomers for 9HZ and 9H10epoZ is eight and sixteen, respectively. However, since 9HZ and 9H10epoZ are oxidation products of 7*epi*Z, where C4 and C7 are in the *R* configuration (Breeden and Coates, 1994; Bleeker *et al.*, 2011), it is safe to assume that this configuration is preserved in 9HZ and 9H10epoZ. This leaves only two possible configurations for 9HZ (*R4,R7,S9* or *R4,R7,R9*) and four for 9H10epoZ (*R4,R7,S9,R10*; *R4,R7,S9,S10*; *R4,R7,R9,R10* and *R4,R7,R9,S10*). The NMR data did not allow us to determine the absolute configuration of 9HZ and 9H10epoZ. In the absence of crystals for X-ray spectroscopy, we addressed this issue by two modelling approaches. The first consists of the comparison of circular dichroism (CD) spectra simulated by quantum chemical calculations with the actual measured spectra, and the second involves substrate-docking simulations on a modelled 3D structure of ShZO in order to find the biochemically supported configurations of the derivatives.

For 9HZ, the calculated CD spectra for the *R4,R7,R9* configuration did not fit the experimental spectra and could be rejected (Figure S13a). Therefore the only configuration

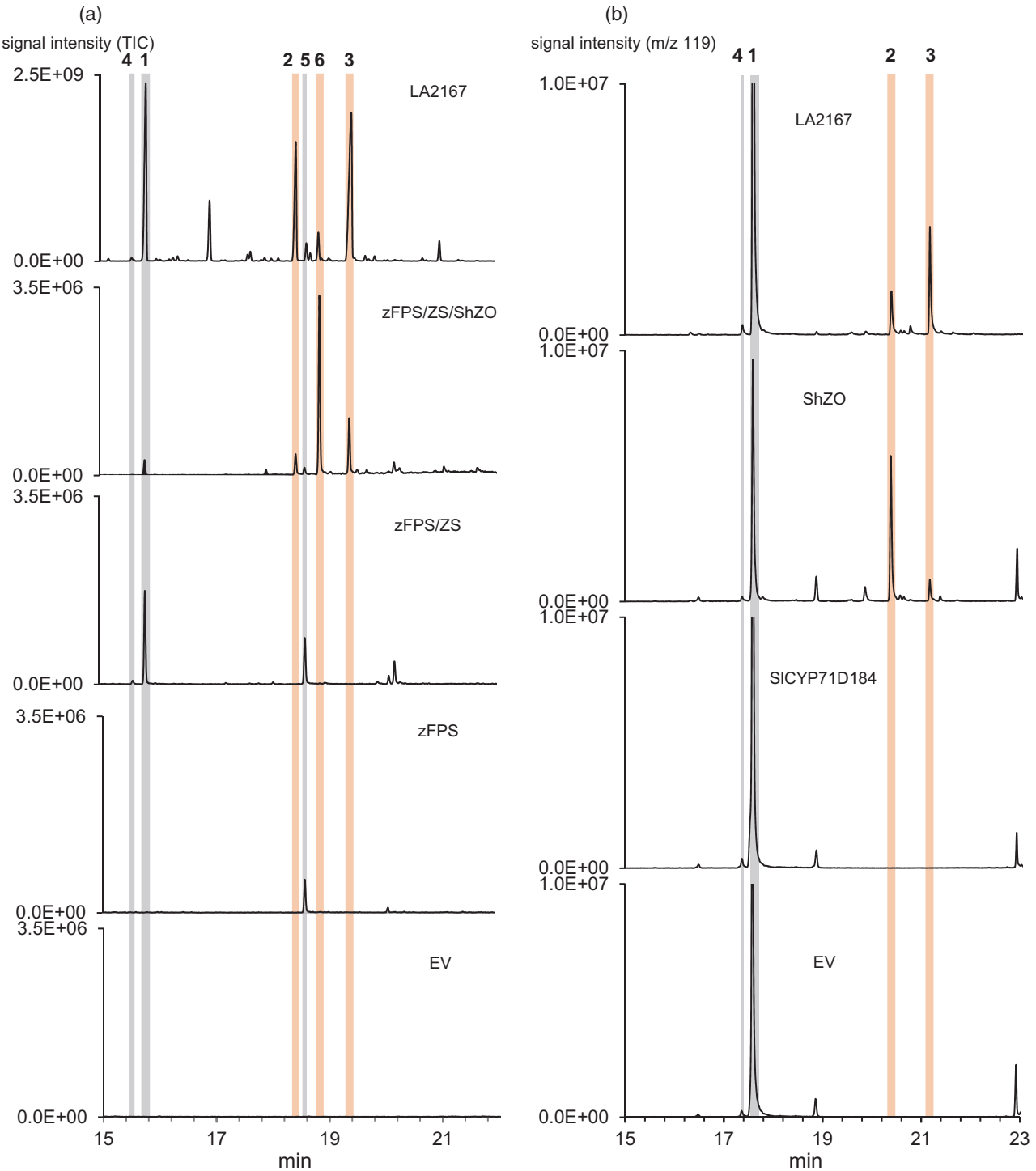

Figure 4. ShCYP71D184 oxidizes 7-*epi*-zingiberene (7*epi*Z) to 9-hydroxy-zingiberene (9HZ) and 9-hydroxy-10,11-epoxyzingiberene (9H10epoZ).
(a) Transient expression in *Nicotiana benthamiana*. The gene combinations indicated at the right of each chromatogram were agroinfiltrated in *N. benthamiana* and leaf extracts analysed by gas chromatography-mass spectrometry (GC-MS). The portion of the total ion chromatograms (TIC) covering sesquiterpenes is shown. LA2167, leaf surface extracts of *Solanum habrochaites* LA2167. zFPS, *cis,cis*-farnesyl diphosphate synthase; ZS, zingiberene synthase; ShZO, ShCYP71D184 (zingiberene oxidase); EV, empty T-DNA vector.
(b) *In vitro* enzyme assays with purified 7*epi*Z. Reactions of microsomes from yeast strains expressing ShZO, SlCYP71D184 or with an EV incubated with purified 7epiZ were analysed by GC-MS (extracted $m/z = 119$). The temperature programme for GC-MS differed between the *N. benthamiana* and microsome assays (see Experimental Procedures). Mass spectra of the products are shown in Figure S12. The detected compounds are labelled as follows. 1, 7*epiZ;* 2, 9HZ; 3, 9H10epoZ ; 4, *ar*-curcumene; 5, farnesol; 6, unknown compound, tentatively identified as 9-hydroxy-10,11-epoxy-*ar*-curcumene.

possible for 9HZ is *R4,R7,S9*. Consequently, only two configurations (*R4,R7,S9,R10* and *R4,R7,S9,S10*) should be possible for 9H10epoZ. However, both these configurations had calculated CD spectra that were in good agreement with the measured ones and could not be rejected (Figure S14).

Next, we generated a 3D structural model of ShZO and used it to perform substrate docking simulations with 7*epi*Z and 9HZ. The structure of the protein model used is shown in Figure S15. Systematic docking studies with both compounds (9HZ and 9H10epoZ) with all configurations tested for the CD spectra simulations were carried out (*R4* stays fixed), including equatorial as well as axial orientation of the side chain with respect to the ring system. Docking studies with all possible stereoisomers of zingiberene show that the *R4,R7* (i.e. 7*epi*Z) configuration is the only one adopting a docking pose with a short distance between a hydrogen atom bound to C9 (H9) and the reactive oxygen atom bound to the heme (Figure 5a). In all other configurations, docking arrangements with the cyclohexadiene ring moiety in proximity to the heme do not allow oxidation at C9. This is caused by the shape of the hydrophobic binding pocked formed mainly by L96, F97, F268, A272, M342 and I454, (Figure 5a). In the case of the docked 7*epi*Z, the pro*S*-H9 is at a distance of 2.5 Å, whereas the proR-H9 is at a distance of 3.9 Å. Thus, the formation of *4R,7R,9S*-hydroxy-zingiberene is highly favoured, confirming the results of the CD spectra measurements. Next, the docking studies with the stereoisomers of 9HZ as a substrate provided strong support for the absolute configuration of 9H10epoZ. Only in the case of the *4R,7R,9S* configuration does the docking pose allow oxidation at the C10 atom, in exactly the same orientation as that found for 7*epi*Z (Figure 5b). As a result, the orientation of the butene moiety, fixed by the restriction of accessible space caused by the spatially neighbouring L208, leaves the formation of 4*R*,7*R*,9*S*,10*S* 9H10epoZ as the only possible outcome (Figure 5c).

In summary, the docking studies confirm *4R,7R,9S*-9HZ and provide strong support for *4R,7R,9S*,10*S*-9H10epoZ as the products of ShZO and 7*epi*Z derivatives found in LA2167 trichomes (Figure 5d–f).

9-Hydroxy-10,11-epoxyzingiberene exhibits toxicity against whiteflies

Next, we sought to evaluate the activity of these zingiberene derivatives towards whiteflies (*B. tabaci*). Whiteflies cause important damage to a number of crops, including tomato, because they are vectors of over 100 plant viruses (Jones, 2003). To investigate the insecticidal properties of 7*epi*Z and its derivatives, a series of no-choice whitefly bioassays were conducted using a realistic range of concentrations of the different fractionated compounds applied to cultivated tomato leaf discs. The concentrations used were based on the quantities measured on the surface of *S. habrochaites* leaves (1–50 μg cm^{-2} for 7*epi*Z and 0.4–12 and 0.4–5 μg cm^{-2} for 9HZ and 9H10epoZ, respectively). Whiteflies were then placed in small cages with one treated leaf disc for 48 h, after which the proportion of surviving whiteflies per cage was determined (Dataset S4). Surprisingly, 7*epi*Z did not affect whitefly survival, even when applied at relatively high concentrations (Figure 6). In contrast, 9H10epoZ caused a significant and concentration-dependent reduction in whitefly survival (ANOVA, least significant difference post-hoc $P < 0.01$). This effect, however, was not found for 9HZ (Figure 6) and appears therefore to be a very specific response to 9H10epoZ. To evaluate further the toxicity of 7*epi*Z, 9HZ and 9H10epoZ on whiteflies, we performed no-choice survival assays on five selected individual F_2 plants from a cross between *S. habrochaites* PI127826 and *S. lycopersicum* cv. Moneymaker, which has a sesquiterpene profile highly similar to that of LA2167. This population was described previously by Bleeker *et al*. (2012). Four of the five tested F_2 lines were homozygous for ShZO and produced varying amounts of 7epiZ, 9HZ and 9H10epoZ, while one line was homozygous for SlCYP71D184 and only produced 7epiZ (Figure S16). Survival of whiteflies showed a significant negative correlation only in the case of 9H10epoZ ($r^2 = 0.72$; $P = 0.016$) (Figure S17).

7-*Epi*-zingiberene and its derivatives have moderate antimicrobial activities

To evaluate the activity of 7*epi*Z, 9HZ and 9H10epoZ against microorganisms, we performed growth inhibition assays with the bacterium *Bacillus subtilis,* the oomycete *Phytophthora infestans* and the fungi *Botrytis cinerea* and *Zymoseptoria triticii*. Microorganisms were grown in the presence of different concentrations of the compounds, and the half-maximum inhibitory concentration, or IC_{50} value, was calculated by comparison with growth under control conditions (Figure S18). Assays with concentrations around 50 μM gave the most significant differences and are shown in Figure 7.

All three compounds display growth inhibition activities against *B. subtilis*, with the strongest effect for 9H10epoZ (Figure 7a). Calculated IC_{50} values were 10.5, 13.6 and 34.6 μM for 9H10epoZ, 9HZ and 7*epi*Z, respectively. In contrast, in the assays with *P. infestans* only 9H10epoZ proved significantly active with an IC50 value of 55.8 μM, while 9HZ provided inhibition only at the highest concentration (200 μM) and 7*epi*Z had no inhibitory effect (Figures 7b and S18). For *Z. triticii* a similar picture emerged, with 9H10epoZ being the most active compound with an IC50 of 33.0 μM (Figures 7c and S18). Finally, against *Botrytis cinerea* (Figure 7d) 9H10epoZ was again the most active compound with an IC50 of 21 μM, while 9HZ and 7-*epi*Z displayed an IC50 of 33.9 and 43.1 μM, respectively.

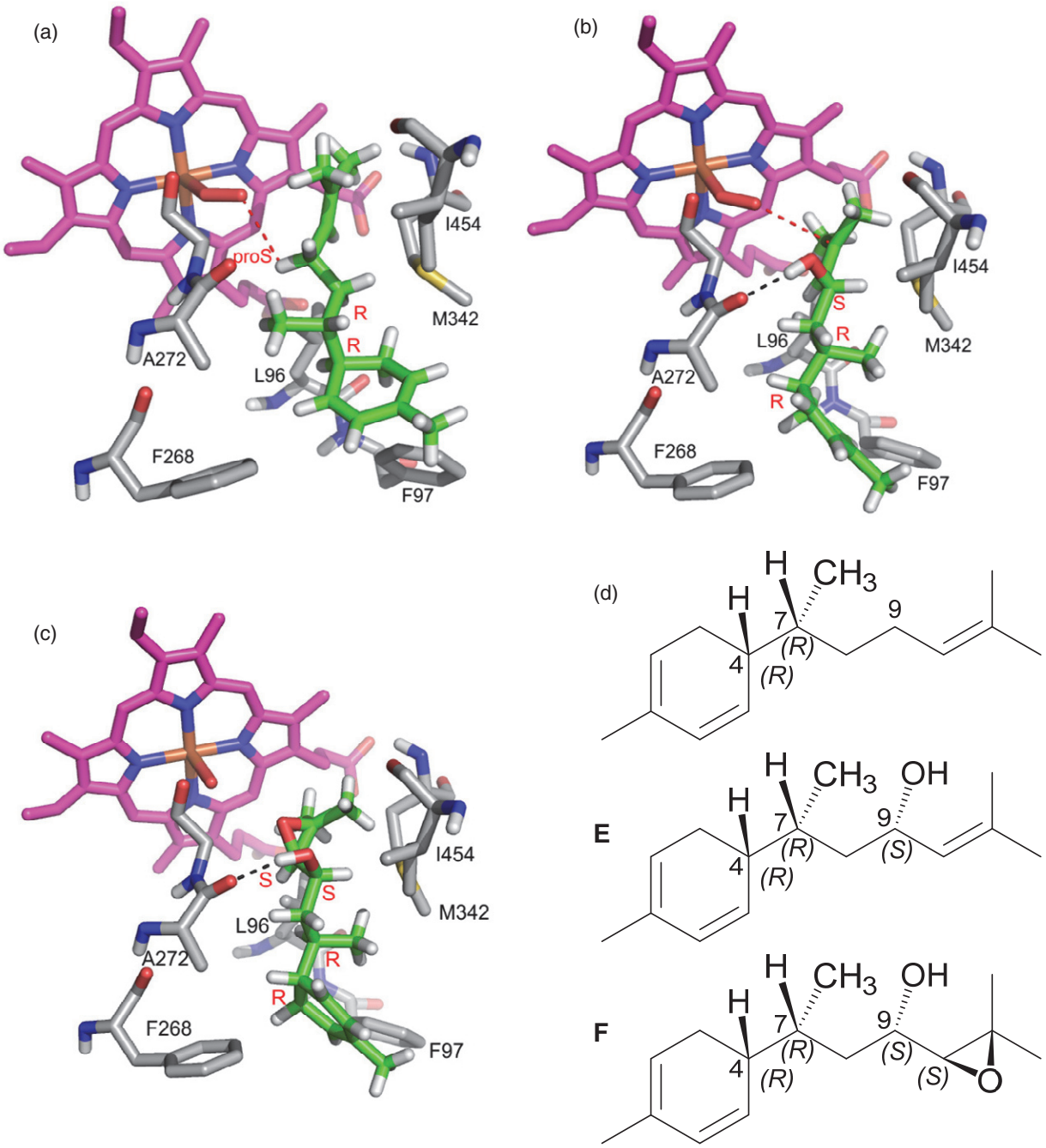

Figure 5. Determination of the absolute configuration of 9-hydroxy-zingiberene (9HZ) and 9-hydroxy-10,11-epoxyzingiberene (9H10epoZ) by molecular docking. The only possible docking arrangement of (*4R,7R*)-zingiberene to the active site of ShZO (ShCYP71D184) from *Solanum habrochaites* LA2167 is shown in (a). The pro*S* 9-hydrogen atom is in close proximity (2.5 Å, red dotted line) to the reactive oxygen atom bound to the heme, favouring the formation of (*4R,7R,9S*)-9-hydroxy-zingiberene. The only possible docking pose of (*4R,7R,9S*)-9-hydroxy-zingiberene to the active site of ShZO is shown in (b). It is in good agreement with the docking pose calculated independently for (*4R,7R*)-zingiberene. The reactive oxygen atom bound to heme is in close proximity (3.4 Å) to the C10 carbon atom to favour the formation of the epoxide with *S10* only. (c) (*4R,7R,9S,10S*)-9-hydroxy-10,11-epoxy-zingiberene formed in the active site. (d) (*4R,7S*)-zingiberene. (e) (*4R,7R,9S*)-9-hydroxy-zingiberene. (f) (*4R,7R,9S,10S*)-9-hydroxy-10,11-epoxy-zingiberene.

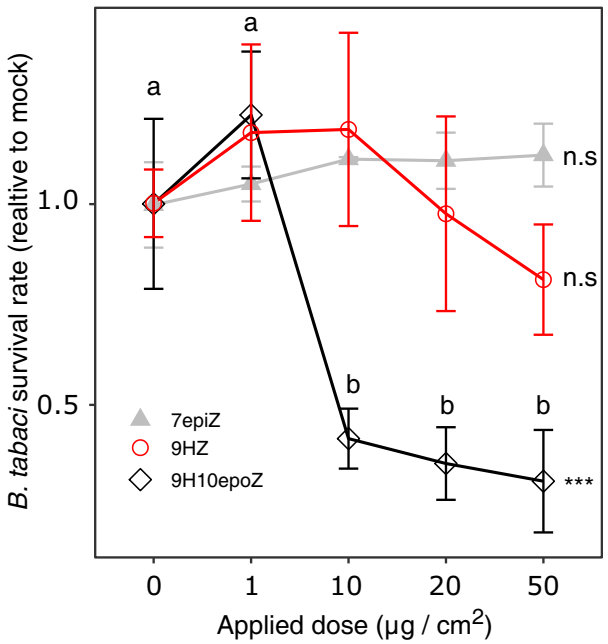

Figure 6. Whitefly toxicity assays of (*4R,7R*)-zingiberene and its oxidized derivatives.
Whitefly survival rates after 48 h on leaf discs treated with different concentrations of 7-*epi*-zingiberene (7epiZ), 9-hydroxy-zingiberene (9HZ) and 9-hydroxy-10,11-epoxyzingiberene (9H10epoZ). The survival rates on treated leaf discs were normalized to the mean survival of the mock treatment (0 µg cm^{-2}). Individual data points represent the average relative survival rate over five leaf discs ± SE. Letters display the statistically significant groups according to Tukey's honestly significant difference post-hoc test after ANOVA comparing the survival rates between the doses of applied metabolite. ANOVA results: n.s., no significant effect; ***$P < 0.001$.

DISCUSSION

In this work we identified two derivatives of 7epiZ, namely 9HZ and 9H10epoZ, and the gene encoding ShZO (ShCYP71D184), a cytochrome P450 monooxygenase enzyme responsible for the biosynthesis of these two sesquiterpenoids in *S. habrochaites* LA2167. We further evaluated the biological activity of these sesquiterpenoids and found that 9H10epoZ in particular showed relevant activity against whiteflies and several microorganisms, including plant pathogens.

The absolute configuration of 9HZ and 9H10epoZ

Given that 9HZ and 9H10epoZ have three and four stereo centres, respectively, determining the absolute configuration is relevant because biological activity is frequently restricted to one or few stereoisomers (Evidente *et al.*, 2013). For example, aggregation pheromones of the marmorated stink bug are two zingeberenol derivatives of a specific configuration (1*S*,4*S*,7*R*,10*S* and 1*R*,4*S*,7*R*,10*S*) with an epoxide between positions 10 and 11, as in 9H10epoZ (Khrimian *et al.*, 2015). In the case of 9HZ and 9H10epoZ, we knew already that their precursor, 7*epiZ*, has the 4*R*,7*R* configuration (Breeden and Coates, 1994; Bleeker *et al.*, 2011). Therefore, given that there are no structural rearrangements in 9HZ and 9H10epoZ, this reduces the number of possible configurations to two and four for 9HZ and 9H10epoZ, respectively. In the absence of crystals, we inferred the absolute configuration of 9HZ and 9H10epoZ by a combination of modelling the CD spectra and docking 9HZ in the active site of ShZO. The comparison of quantum chemical calculated and measured CD spectra has recently become a valuable alternative method for determining the absolute configuration of small molecules, particularly in the pharmaceutical industry (Polavarapu, 2016). In the case of 9HZ, of the two possible configurations, only the *4R,7R,9S* gave a fitting CD spectrum (Figure S11b). This was confirmed by the docking of 9HZ in the active site of the modelled ShZO. In the case of 9H10epoZ, the CD spectra could not distinguish between the two remaining possible configurations, but the docking study strongly argued for the *4R,7R,9S,10S* configuration (Figure 5c). We are, however, aware that the support for these configurations is indirect and that direct demonstration of their absolute configuration would require chemical synthesis or crystallization, as requested by the Metabolomics Standards Initiative guidelines (Sumner *et al.*, 2007).

ShZO belongs to a clade of CYPs sequentially oxidizing sesquiterpenes

ShZO belongs to a clade of CYP71D enzymes from the Solanaceae that includes two characterized sesquiterpene oxidases, premnaspirodiene oxygenase (HPO, CYP71D55) and *epi*-aristolochene 1,3-dihydroxylase (EAH, CYP71D20) (Figure S9) (Ralston *et al.*, 2001; Takahashi *et al.*, 2007). Notably, both of these CYP enzymes carry out two sequential oxidations like ShZO, at a single position for HPO resulting in the formation of a keto group or at two positions for EAH leading to the formation of a di-alcohol. Premnaspirodiene oxygenase was also shown to oxidize other sesquiterpene substrates including *epi*-aristolochene (Takahashi *et al.*, 2007). Substrate promiscuity seems to be a common feature of CYP enzymes in plant specialized metabolism, as also shown in diterpenoid biosynthesis (Bathe *et al.*, 2019). It would therefore be of interest in future studies to evaluate the spectrum of sesquiterpene substrates that can be oxidized by ShZO.

From a volatile signalling molecule to a toxic derivative

The bioactivity assays performed here point to a specific toxicity of 9H10epoZ, for which a clear, concentration-dependent effect was observed against *B. tabaci* (Figure 6). A recent study also identified 9HZ and 9H10epoZ as potent repellents of spider mites, *Tetranychus urticae* (Dawood and Snyder, 2020), further confirming these compounds to be of potential relevance for resistance against arthropod

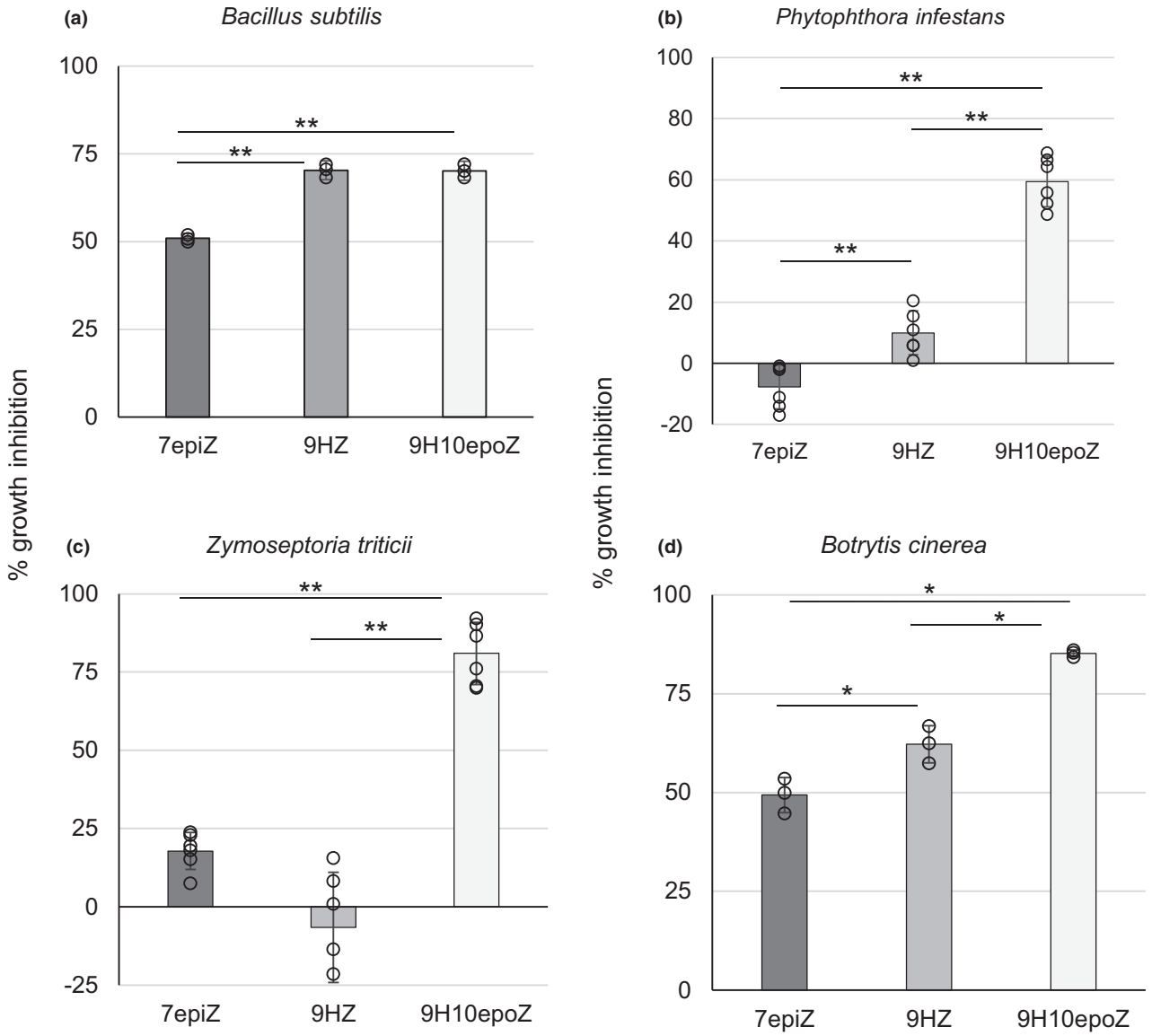

Figure 7. Growth inhibition assays of 7-*epi*-zingiberene (7epiZ), 9-hydroxy-zingiberene (9HZ) and 9-hydroxy-10,11-epoxyzingiberene (9H10epoZ) against various microorganisms.

Graphs display the percentage of growth inhibition (y-axis) compared with positive controls after 7 days of incubation for (b)–(d) and 15 h of incubation for (a). *Bacillus subtilis* (a), *Phytophthora infestans* (b), *Zymoseptoria tritici* (c) and *Botrytis cinerea* (d) were grown in liquid cultures with concentrations of 7*epiZ*, 9HZ and 9H10epoZ ranging from 1 to 100 μM for (a), and from 0.52 to 42 μg ml^{-1} for (b)–(d). The data shown here are 50 μm for (a) and 14 μg ml^{-1} for (b)–(d). Statistical differences between groups were evaluated by ANOVA followed by a two-sample *t*-test with unequal variances (*$P < 0.05$; **$P < 0.01$).

pests. We would like to point out here that the identification of 9HZ and 9H10epoZ by Dawood and Snyder is based on a patent application that we submitted in 2015 and subsequently withdrew (Zabel and Tissier, 2015). The concentrations of the zingiberenoids we used here are in line with those present on the leaf surface of *S. habrochaites*. According to our calculations based on the measured quantities of sesquiterpenoids and the volume of the type VI trichomes, we estimate that concentration of each sesquiterpenoid in LA2167 trichomes is around 1 M (see Data S1). This suggests that high concentrations of these compounds are released locally when type VI trichomes are damaged by herbivores or during pathogen infection. *Solanum habrochaites* LA2167 produces both a repellent (7*epiZ*) (Bleeker *et al.*, 2011) and a compound that is toxic to whiteflies. Whereas it was previously assumed that

volatile sesquiterpenes from wild tomato inform the insect about the presence of lethal doses of the compound prior to landing (Bleeker *et al.*, 2011), here we show that 7*epi*Z, even at high concentrations, is not toxic to *B. tabaci*. Instead, the repellent volatile may signal the presence of a toxic derivative on the leaf surface. However, we previously showed that 7*epi*Z is toxic to spider mites using transgenic tomato lines that do not produce derivatives (Bleeker *et al.*, 2012), further underlining the insect specificity of individual metabolites. In light of this, determining the absolute configuration is relevant because biological activity is frequently restricted to only one or a few stereoisomers. For example, while 7*epi*Z and *R*-curcumene are repellent to whiteflies, α-zingiberene and *S*-curcumene (isomers found in ginger and basil, for example) do not have such an effect (Bleeker *et al.*, 2011).

Furthermore, the 7*epi*Z derivatives, 9H10epoZ in particular, also showed moderate antimicrobial activity against several microorganisms, including important pathogens like *B. cinerea* and *P. infestans* (Figure 7). *Botrytis cinerea* and *P. infestans* are known tomato pathogens but *Z. triticii* is not. Thus, the antimicrobial activity of 9H10epoZ does not seem to be specifically directed against tomato pathogens. Quantitative resistance to *P. infestans* was found in different accessions of *S. habrochaites* with quantitative trait loci (QTLs) located on chromosomes 11 and 5 (Johnson *et al.*, 2012; Haggard *et al.*, 2013, 2014; Copati *et al.*, 2019). Accession LA2167 was not included in those studies, and it is still unknown whether the quantitative resistance identified there was based on specialized metabolites. Although this putative contribution of plant-produced sesquiterpenes to quantitative resistance to microbial pathogens is of major interest, it remains debatable whether this antimicrobial activity by trichome-produced metabolites is relevant in a field environment. Lu *et al.* (2013) showed that levels of artemisinin and dihydroartemisinic acid in the glandular trichomes of *Artemisia annua* enhance resistance to *B. cinerea*, demonstrating that indeed metabolites stored in glandular trichomes can contribute to pathogen resistance. Thus, further investigations on a putative contribution of sesquiterpenes of LA2167 to quantitative resistance against microbial pathogens should be carried out in the future.

Genes for tomato zingeberenoid biosynthesis as markers for insect resistance

The clear toxicity of 9H10epoZ towards whiteflies and spider mites makes the genes encoding ShZO, zFPS and ShZIS potential molecular markers for breeding insect resistance from *S. habrochaites* into the cultivars of *S. lycopersicum*. Breeding metabolite-based insect resistance from wild tomato species into cultivated tomato has proven challenging, essentially because of the highly polygenic nature of these traits. There are several reasons for the requirement for multiple genes. The first is that several genes are required for the biosynthesis of compounds produced by the glandular trichomes at the leaf surface and they typically localize to different regions of the genome. Our work here provides such an example, because the genes for the synthesis of 7*epi*Z are clustered on chromosome 8 (Sallaud *et al.*, 2009; Bleeker *et al.*, 2012) while *ShZO* is on chromosome 1. Other examples are the acylsugars, which provide strong resistance against a variety of arthropod pests (Lemke and Mutschler, 1984; Goffreda and Mutschler, 1987; Goffreda *et al.*, 1989; Hawthorne *et al.*, 1992; Ben-Mahmoud *et al.*, 2018, 2019). Quantitative trait locus mapping studies have shown the involvement of multiple loci (Mutschler *et al.*, 1996; Blauth *et al.*, 1999; Leckie *et al.*, 2012, 2013, 2014). Additionally, studies on the biosynthesis of acylsugars showed that several acyltransferases are involved that are found at different chromosome locations (Schilmiller *et al.*, 2012, 2015; Fan *et al.*, 2016). Secondly, as mentioned earlier, these metabolites are produced and stored in specialized structures. Therefore, additional factors including trichome type, density and productivity need to be considered. There is strong support for a positive correlation between the level of resistance and the density of trichomes, which need to be of the correct type producing the compounds that are involved in resistance. Tomato has four different types of glandular trichomes, with type I/IV producing acyl sugars and type VI terpenoids. A number of genes involved in the development of type VI trichomes have been identified (Schuurink and Tissier, 2020), but to the best of our knowledge, the genes controlling their density are not yet known. Quantitative trait locus analysis in crosses between *Solanum galapagense* and *S. lycopersicum* allowed the identification of a major locus on chromosome 2 contributing to both insect resistance and type IV trichome density together with the production of acyl sugars, but the genes remain to be identified (Firdaus *et al.*, 2013; Vosman *et al.*, 2019). Yet another aspect is the capacity to produce and accumulate sufficiently large quantities of specialized metabolites in trichomes. In some *S. habrochaites* accessions sesquiterpenoids produced by type VI trichomes can represent more than 10% of the leaf dry weight (Frelichowski and Juvik, 2005), which is explained not only by the higher density of trichomes but by the fact each trichome produces significantly more terpenes than in cultivated tomato (Balcke *et al.*, 2017). This could be due to the level of expression of the biosynthesis genes (Ben-Israel *et al.*, 2009) but also to the capacity of type VI trichomes to store the metabolites in a cavity located between the glandular cells (Bergau *et al.*, 2015; Bennewitz *et al.*, 2018).

In conclusion, we identified 7*epi*Z oxidation products and the enzyme responsible for their biosynthesis from an accession of the wild tomato *S. habrochaites*. This information can be used to breed tomato lines with improved

performance against pests by reconstituting the whole pathway by classical breeding, transgenesis or CRISPR-Cas9-based knock-in technology (Dahan-Meir *et al.*, 2018). Of these, the CRISPR-Cas9 approach is probably the most promising as it should lead to optimal gene expression levels and avoid the introgression of large chromosomal fragments around the genes of interest from *S. habrochaites,* which can lead to negative side-effects.

EXPERIMENTAL PROCEDURES

Plant material and growth

Seeds of *S. habrochaites* accessions LA2167, LA1777, LA1753, LA2650, LA2556 and *S. lycopersicum* accession LA4024 were obtained from the Tomato Genetics Resource Center at UC Davis (http://tgrc.ucdavis.edu/). *Solanum habrochaites* accession PI 127826 was obtained from USDA Germplasm (https://www.ars-grin.gov/). Plants were grown in a greenhouse under controlled conditions of 25°C and 55% humidity during the day and 20°C and 75% humidity during the night. Plants were illuminated for 16 h (from 06:00 to 22:00) resulting in a light intensity of 5 to 25 klux depending on the weather conditions. The plants were watered once a week with a fertilizer solution (0.1% Kamasol Brilliant Blau, Compo Expert GmbH, http://www.compo-expert.com/).

Trichome harvest

Leaves from 5–6-week-old plants were cut at their base and immediately brushed several times across their surface with a paintbrush dipped in liquid N_2 while keeping them above a mortar containing liquid N_2. The collection of trichomes from 20–30 leaves was sufficient to extract total RNA for cDNA synthesis. The harvested material was filtered through a steel sieve of 150 μm diameter (Atechnik, https://www.atechnik.net/) to further separate the isolated glandular trichomes from leaf debris and to eliminate non-glandular trichomes. After N_2 evaporation, the collected trichomes were transferred with a cooled down spatula into a 1.5 ml reaction tube and stored at −80°C until further processing.

Genomic DNA, RNA isolation and cDNA synthesis

Genomic DNA from tomato plants was extracted with a Qiagen DNeasy Plant Mini Kit (http://www.qiagen.com/) following the manufacturer's instructions. The RNA isolation of leaf and trichome material from tomato plants was done using an RNeasy Mini Kit (Qiagen). The RNA concentration was measured with a Nanodrop spectrophotometer (Thermo Fisher Scientific, http://www.thermofisher.com/) and the quality of the RNA was checked with a QIAxcel Advanced system (Qiagen). A DNase I digest was done using the Ambion DNA-free™ kit (Life Technologies, https://www.thermofisher.com/). Subsequently, cDNA synthesis was done using a RevertAid H Minus-MuLV reverse transcriptase kit (Thermo Fisher Scientific) according to the manufacturer's instructions with 1 μg of input RNA.

Polymerase-chain reaction

For DNA amplification from genomic DNA, cDNA or plasmid DNA for later cloning procedures different PCR methods were used. A KOD Hot Start DNA Polymerase (KOD) (Sigma-Aldrich, http://www.sigmaaldrich.com/), Phusion high fidelity DNA polymerase (Phusion) (New England Biolabs, http://www.neb.com/) and the proofreading DreamTaq DNA-Polymerase (DreamTaq) (Thermo Fisher Scientific) were used following the manufacturers' recommendations. The following PCR programme was applied: an initial denaturation step of 2 min at 95°C followed by 30–35 cycles of 30 sec denaturation at 95°C, a 30 sec annealing step at 55°C and elongation for 0.5 min kb^{-1} (KOD) or 1 min kb^{-1} (DreamTaq) gene length at 72°C with 5 min final extension step at 72°C. Oligonucleotide primers used for PCR amplification are listed in Data S2.

Quantitative real-time polymerase chain reaction

The qRT-PCR analysis was done with a Connect 96x Real-Time PCR system (Bio-Rad, https://www.bio-rad.com/). The input for each reaction was 3 μl of the cDNA reaction mixture diluted 20 times. The reaction was done with the my-Budget 5× EvaGreen QPCR Mix II kit (Bio&Sell, http://www.bio-sell.de/en/). The PCR programme consisted of an initial denaturation step of 15 min at 95°C followed by 40 cycles of 10 sec at 95°C and 20 sec at 55°C. The melt curve was recorded after additional denaturing at 95°C for 30 sec, cooling down to 65°C for 30s and heating up again to 95°C with a ramp rate of 0.1°C sec^{-1}. The complete list of oligonucleotides used is provided in Data S2.

Complementary DNA microarray hybridization

Complementary DNA from leaves of the *S. habrochaites* accessions LA1753, LA2167, LA1777, LA2556 and LA2650 was hybridized to a custom-designed microarray chip and the data were analysed as described in Balcke *et al.* (2017). The data for the three genes used in this study are shown in Figure 3(a). The complete dataset is available online as Dataset S1.

Solanum habrochaites LA2167 × *S. lycopersicum* LA4024 backcross population

To generate a backcross population between accession LA2167 (*S. habrochaites*) and LA4024 (*S. lycopersicum*), pollen from the anthers of the stamen (male) of LA2167 was collected on a glass slide and used to pollinate emasculated flowers of LA4024. This procedure was repeated several times with each pollinated flower over the following 7 days to ensure pollination. The progeny were then analysed by GC-MS and high-resolution melt (HRM) genotyping for at least eight independent loci. Only plants producing 7*epi*Z and its derivatives, and heterozygous for the markers, were considered bona fide F_1 plants and were kept for the backcrosses. Next, pollen from the F_1 plants was used to pollinate LA4024 flowers generating the BC_1F_1 generation. Each BC_1F_1 plant was then individually characterized, genotyped and analysed by GC-MS as for the F_1 plants. Plants that had the phenotype and genotype of LA4024, i.e. resulting from self-fertilization of LA4024, were discarded.

Molecular mapping

For the mapping, 114 markers were used covering all 12 chromosomes (Dataset S2). Of these markers, 89 were iPLEX™ markers and iPLEX™ assays were performed at ATLAS Biolabs (http://www.atlas-biolabs.com/). The other 25 were HRM markers and assays were performed as described in Bennewitz *et al.* (2018). The presence of the different alleles in the BC_1F_1 progeny was correlated to detection of 9HZ and 9H10epoZ in order to determine the chromosomal position of *ShZO* (see Dataset S3).

Leaf surface extracts and analysis by GC-MS

Leaf-surface extracts were collected from six leaflets about 5 cm in length by adding 2 ml *n*-hexane and shaking for 1 min. The hexane was taken off and centrifuged at 16 000 ***g*** for 90 s to remove debris.

One microlitre of the hexane supernatant was then injected in a Trace GC Ultra gas chromatograph coupled to an ISQ mass spectrometer (Thermo Scientific). The GC-MS analyses were performed as described in Brückner *et al.* (2014). Briefly, the exudates were separated on a 30 m × 0.32 mm diameter capillary, with a 0.25 μm film of ZB-5MS from Phenomenex (https://www.phenomenex.com/). Injection was done in splitless mode at 250°C. The GC oven temperature programme was as follows: 50°C for 1 min followed by a linear gradient of 7°C min^{-1} up to 300°C and then 20°C min^{-1} to 330°C. Helium was used as a carrier gas with a flow rate of 1 ml min^{-1} and molecules were ionized using electron ionization at 70 eV. The temperature of the transfer line was 200°C and that of the ion source 250°C. The MS data were recorded from 50 to 450 *m/z*.

High-resolution mass spectrometry

The hexane extracts from *S. habrochaites* LA2167 were dried down and resuspended in methanol. The methanolic extracts were injected onto a EC 150/2 Nucleoshell RP18 column (Macherey-Nagel, http://www.mn-net.com/) using a Dionex Ultimate 3000 UHPLC instrument and analysed by a Orbitrap Elite mass spectrometer (Thermo Fisher Scientific). For detailed information of the high-resolution MS method see Bathe *et al.* (2019).

Purification of 9HZ and 9H10epoZ

Around 500–1000 leaflets of the *S. habrochaites* accession LA2167 were extracted with 500 ml of *n*-hexane for 5 min. The organic solvent was then gently removed by a rotary evaporation at 20°C. The dried sample was then resolved in 50 ml *n*-hexane and stored at −20°C. In parallel a glass column was packed with 15 g CHROMABOND silica adsorbent material (Machery-Nagel) and equilibrated several times with 50 ml *n*-hexane. After preparation the sample was applied to the column. Afterwards the column was washed six times with a 90:10:1 mixture of *n*-hexane:ethyl acetate:methanol. A second elution step was then carried out with a 50:50:1 mixture of *n*-hexane:ethyl acetate:methanol. Fractions of 50 ml were collected and cooled down to 4°C until further analysis.

Nuclear magnetic resonance analysis

The NMR spectra were recorded on an Agilent (Varian, http://www.varian.com/) VNMRS 600 NMR spectrometer at 599.832 MHz (^{1}H, ^{2}D) and 150.826 MHz (^{13}C) using a 5 mm inverse detection cryoprobe. The samples were dissolved in C_6D_6. Chemical shifts were referenced to internal TMS ($\delta^{1}H$ 0 p.p.m.) and internal C_6D_6 ($\delta^{13}C$ 128.0 p.p.m.).

Circular dichroism

The CD spectra of 9HZ and 9H10epoZ were recorded on a JASCO-J815 CD spectrometer (https://jascoinc.com/) using *n*-hexane as the solvent.

Molecular cloning

Golden Gate cloning was used for the preparation of all plasmid constructs reported here (Engler *et al.*, 2008; Weber *et al.*, 2011; Werner *et al.*, 2012; Engler *et al.*, 2014). The complete list of constructs used is provided in Supplemental Data S1. The zFPS coding sequence was codon optimized (see Supplemental Data S1) for *N. benthamiana*, while ShZS (zingiberene synthase) and ShCYP71D184 were amplified as cDNA from LA2167.

Transient expression in *N. benthamiana*

The T-DNA constructs containing cDNAs for zFPS, ShZS, ShZO (CYP71D184) and the Arabidopsis cytochrome P450 reductase (ATR1), all under the control of the 35S promoter (see list of constructs in the Data S1), were transformed into *Agrobacterium tumefaciens* strain GV3101 (pMP90) by electroporation. Cultures of the *A. tumefaciens* strains containing the respective T-DNAs were mixed in different combinations at a final OD_{600} of 0.6. In combinations with fewer genes, the mixture was complemented by the addition of an equivalent amount of an *A. tumefaciens* strain expressing GFP with the 35S promoter. The cells were resuspended in infiltration buffer [5% sucrose (w/v) and 4.3 g L^{-1} Murashige and Skoog basal salt mixture] containing 20 μM acetosyringone. After infiltration the plants were brought back into growth chambers for an additional 5 days, after which they were extracted for GC-MS analysis. The extraction was carried out as in Brückner and Tissier (2013). Six leaf discs of diameter 0.9 cm were cut with a cork borer and extracted in 1 ml hexane in a 1.5 ml tube. After incubation for 5 min, the hexane was transferred to a new tube and centrifuged at 16 000 ***g*** for 5 min. The hexane was then transferred again to a new tube and dried on ice and under a flow of nitrogen. The extract was then resuspended in 200 μl hexane and transferred to a GC vial for injection.

Yeast microsome preparation and *in vitro* enzyme assays

The preparation of microsomal fractions from yeast cells expressing ShCYP71D184 or SlCYP71D184 was carried out as described previously (Scheler *et al.*, 2016). For the *in vitro* assays, the following ingredients were mixed in a 2 ml microtube: 336 μl of 100 mM sodium phosphate (pH 7.4), 214 μl of deionized water, 6 μl of 100 mM NADPH, 2.5 μl of a 25 mM substrate solution in DMSO and 40 μl of microsomes. The reaction was incubated for 2 h at 30°C with gentle shaking (130 r.p.m.). Then 200 μl of *n*-hexane was added to extract the terpenes. After thorough mixing the tubes were centrifuged for 15 sec at 20 000 ***g*** in a benchtop centrifuge. Then 150 μl of the organic phase was transferred to a small insert in a GC vial. The GC-MS conditions were as described above except the GC oven temperature programme was as follows: 50°C for 1 min followed by a linear gradient of 7°C min^{-1} until 185°C and then with 30°C min^{-1} to 320°C.

Computational methods

The computational methods used for modelling the CD spectra, the ShZO 3D structure and the protein–substrate docking studies are described in detail in the Supplemental Information file.

Bemisia tabaci toxicity assay

The fractions purified by solid phase extraction were dried under N_2 and dissolved in 1.7 mM TritonX-100 followed by thorough mixing using a vortex. Twenty microlitres of diluted fraction, containing the appropriate concentration of terpenoids, was applied to the abaxial side of freshly harvested leaf discs (diameter 1.5 cm) from 5-week-old *S. lycopersicum* (cv. Moneymaker) plants. Leaf discs treated with 0–50 μg terpenoids per cm^2 ($n = 5$) were air dried for 30 min prior to starting the experiment. Fifteen whiteflies (*B. tabaci*) were collected from a cucumber rearing and placed in small containers (Greiner analyser cups, 2.9 cm diameter × 5.2 cm height) with a 1 cm diameter opening in the lid. The opening was covered with a leaf disc facing the treated side inside the cup. The leaf disc was subsequently covered with moist filter paper (Whatman) and sealed with Parafilm®. Cages were placed for 48 h in a climate chamber at 24°C after which dead and living whiteflies were counted under a stereomicroscope. The survival rate per cage was determined and, by means of standardizing separate experiments, survival rates were calculated relative to the mean survival of the mock controls. Per metabolite, the survival

rates between the different doses were tested by ANOVA and Tukey's honestly significant difference post-hoc test. Whitefly survival assays on the F_2 plants were performed in clip-cages (Bioquip #1458, http://www.bioquip.com/) attached to fourth fully expanded leaf from the plant apex (n = 6–8). Cages were filled with 15–20 adult whiteflies and the numbers of living and dead whiteflies were recorded after 5 days.

Antibacterial assay

Bacillus subtilis strain 168 expressing yellow fluorescent protein (YFP) was used (Veening *et al.*, 2004). The fluorescence was recorded as a 'benchmark' for the growth inhibition induced by the test compounds, as described by Michels *et al.* (2015). *Bacillus subtilis* was grown on TY medium with 1% tryptone, 0.5% yeast extract, 1% NaCl and chloramphenicol (5 μg ml^{-1}) for selection. The cell density was adjusted to 1.6×10^5 cells ml^{-1} resuspended afterwards in 10 ml of fresh TY medium. The assay was done for three biological replicates in black flat-bottomed 96-well microtitre plates containing the cell suspensions with added methanol extracts of 7*epiZ*, 9HZ or 9H10epoZ. Autofluorescence of the single compounds (K1, n = 1) in TY medium, of the bacterial suspension alone (K2, n = 6) and of the reference control (a mixture of pure methanol and inoculum) (K3, n = 6), which served as reference for 100% growth, was measured. Finally, K4 was a positive control containing erythromycin, a common antibiotic, which was dissolved in pure methanol. The fluorescent measurement was done with a microtitre plate reader Tecan GENios Pro (https://lifesciences.tecan.com/) (λ_{ex} = 510 nm, λ_{em} = 535 nm, bandwidth = 10 nm, gain 45, 60, 10 flashes, integration time 40 μsec, 50% mirror, 3 × 3 quadratic measurements per well, temperature 27°C, shaking 10 sec low intensity, settle time 1 sec) at the time point $t = 0$ (t_0) after inoculation with *B. subtilis* and again under the same specifications after 15 h (t_{15}) incubation at 30°C. Calculations of the percentage of growth inhibition relative to K3 were done using the following equation: growth inhibition (%) = $\{1 - 100[x_{sample}(t_{15} - t_0)/x_{k3}(t_{15} - t_0)]\} \times 100$.

Assays for growth inhibition of plant pathogens

Growth inhibition assays with *B. cinerea* Pers., *Septoria tritici* Desm. and *P. infestans* Mont. were performed in 96-well microtitre plates. The experimental setup was done according the Fungicide Resistance Action Committee (www.frac.info/). Here, 7*epiZ*, 9HZ or 9H10epoZ were tested by adding a dilution series of a stock solution (0.52–42 μg ml^{-1} in DMSO, final DMSO concentration 2.5%) to the assay. Pyraclostrobin (Sigma-Aldrich), a commercially available fungicide, was used as a positive control for growth inhibition. For each concentration three biological replicates were measured. Pathogenic growth was determined by measuring the optical density (λ = 405 nm) 7 days after inoculation with a GENios Pro microtiter plate reader (Tecan) doing five measurements per well, using multiple reads with 3 × 3 quadratic measurements per well.

ACKNOWLEDGEMENTS

We would like to thank the Leibniz Institute of Plant Biochemistry (IPB) for funding this project and the greenhouse personnel of the IPB (Petra Jansen, Philip Plato and Sabine Voigt) for taking care of the plants. Open Access funding enabled and organized by ProjektDEAL.

AUTHOR CONTRIBUTIONS

The project was conceived and supervised by AT. SZ performed the identification and purification of the zingiberene derivatives, generated the backcross population, analysed the BC_1F_1 plants by GC-MS and carried out the molecular mapping and all the cloning and the transient expression in *N. benthamiana*. WB did the CD spectrum simulation and the 3D protein modelling and docking. AP performed the NMR analysis. BA provided support for the design of molecular markers. RK and PB performed the whitefly assays. AT wrote the manuscript, which all authors revised and approved.

CONFLICT OF INTEREST

The authors declare no conflict of interest.

DATA AVAILABILITY STATEMENT

The cDNA sequence of *ShZO* was deposited on GenBank under the accession MT786523. All biological materials described here will be provided upon request to AT.

SUPPORTING INFORMATION

Additional Supporting Information may be found in the online version of this article.

Dataset S1. Microarray data of trichomes from *Solanum habrochaites* accessions LA1753, LA2167, LA2556, LA2650 and LA1777.

Dataset S2. List of molecular markers used for the genotyping of the *Solanum habrochaites* LA2167 × *Solanum lycopersicum* LA4024 backcross population.

Dataset S3. Chromosome mapping data for the *Solanum habrochaites* LA2167 × *Solanum lycopersicum* LA4024 backcross population.

Dataset S4. Results of the *Bemisia tabaci* toxicity assays.

Figure S1. Electrospray ionization-MS of trimethylsilylated compounds 2 (a) and 3 (b).

Figure S2. Theoretical MS fragmentation ions of trimethylsilylated compound 2.

Figure S3. Theoretical MS fragmentation ions of trimethylsilylated compound 3.

Figure S4. Purification of zingiberene derivatives from *Solanum habrochaites* LA2167.

Figure S5. High-resolution MS of compound 2.

Figure S6. High-resolution MS of compound 3.

Figure S7. Key ^1H, ^{13}C HMBC (H to C) and $^1H,^1H$ COSY correlations of 9-hydroxyzingiberene (9HZ).

Figure S8. Gas chromatography-MS total ion chromatograms of leaf surface extracts from several *Solanum habrochaites* accessions and mass spectra of selected compounds.

Figure S9. Alignment of the amino acid and coding sequences of ShCYP71D184 and ShCYP71D184 (=ShZO).

Figure S10. Phylogenetic tree of cytochrome P450 oxygenase sequences related to ShCYP71D184 (=ShZO).

Figure S11. Mass spectra of zingiberene and derivatives produced in *Nicotiana benthamiana*.

Figure S12. Gas chromatography MS chromatograms of *in vitro* enzyme assays with 9-hydroxy-zingiberene as substrate and mass spectra of substrate and product.

Figure S13. Comparison of calculated Boltzmann-weighted circular dichroism spectra (red lines) with the experimental one (black line) of four hydroxy-zingiberene configurations.

Figure S14. Comparison of calculated Boltzmann-weighted circular dichroism spectra (red lines) with the experimental one (black line) of 9-hydroxy-10,11-epoxy-zingiberene configurations.

Figure S15. Tertiary structure of *Solanum habrochaites* zingiberene oxidase.

Figure S16. Levels of 7-*epi*-zingiberene and derivatives in *Solanum habrochaites* PI127826, *Solanum lycopersicum* cv. Moneymaker and selected F_2 plants from a cross between PI127828 and Moneymaker.

Figure S17. No choice survival assays of *Bemisia tabaci* on *Solanum habrochaites* PI127826, *Solanum lycopersicum* cv Moneymaker and selected F_2s from a cross between PI127826 and Moneymaker.

Figure S18. Growth inhibition assays of 7-*epi*-zingiberene, 9-hydroxy-zingiberene and 9-hydroxy-10,11-epoxy-zingiberene against various microorganisms.

Data S1. List of plasmids used in this study.

Data S2. List of oligonucleotides used for cloning and quantitative real-time PCR.

REFERENCES

Balcke, G.U., Bennewitz, S., Bergau, N., Athmer, B., Henning, A., Majovsky, P., Jiménez-Gómez, J.M., Hoehenwarter, W. and Tissier, A. (2017) Multi-omics of tomato glandular trichomes reveals distinct features of central carbon metabolism supporting high productivity of specialized metabolites. *Plant Cell*, **29**, 960–983.

Bathe, U., Frolov, A., Porzel, A. and Tissier, A. (2019) CYP76 oxidation network of abietane diterpenes in Lamiaceae reconstituted in yeast. *J. Agric. Food Chem.* **67**, 13437–13450.

Ben-Israel, I., Yu, G., Austin, M.B., Bhuiyan, N., Auldridge, M., Nguyen, T., Schauvinhold, I., Noel, J.P., Pichersky, E. and Fridman, E. (2009) Multiple biochemical and morphological factors underlie the production of methylketones in tomato trichomes. *Plant Physiol.* **151**, 1952–1964.

Ben-Mahmoud, S., Anderson, T., Chappell, T.M., Smeda, J.R., Mutschler, M.A., Kennedy, G.G., De Jong, D.M. and Ullman, D.E. (2019) A thrips vector of tomato spotted wilt virus responds to tomato acylsugar chemical diversity with reduced oviposition and virus inoculation. *Sci. Rep.* **9**, 17157.

Ben-Mahmoud, S., Smeda, J.R., Chappell, T.M., Stafford-Banks, C., Kaplinsky, C.H., Anderson, T., Mutschler, M.A., Kennedy, G.G. and Ullman, D.E. (2018) Acylsugar amount and fatty acid profile differentially suppress oviposition by western flower thrips, *Frankliniella occidentalis*, on tomato and interspecific hybrid flowers. *PLoS One*, **13**, e0201583.

Bennewitz, S., Bergau, N. and Tissier, A. (2018) QTL mapping of the shape of type VI glandular trichomes in tomato. *Front. Plant Sci.* **9**, 1421.

Bergau, N., Bennewitz, S., Syrowatka, F., Hause, G. and Tissier, A. (2015) The development of type VI glandular trichomes in the cultivated tomato *Solanum lycopersicum* and a related wild species *S. habrochaites*. *BMC Plant Biol.* **15**, 289.

Blauth, S.L., Steffens, J.C., Churchill, G.A. and Mutschler, M.A. (1999) Identification of QTLs controlling acylsugar fatty acid composition in an intraspecific population of *Lycopersicon pennellii* (Corr.) D'Arcy. *Theor. Appl. Genet.* **99**, 373–381.

Bleeker, P.M., Diergaarde, P.J., Ament, K. *et al.* (2011) Tomato-produced 7-epizingiberene and *R*-curcumene act as repellents to whiteflies. *Phytochemistry*, **72**, 68–73.

Bleeker, P.M., Mirabella, R., Diergaarde, P.J., VanDoorn, A., Tissier, A., Kant, M.R., Prins, M., de Vos, M., Haring, M.A. and Schuurink, R.C. (2012) Improved herbivore resistance in cultivated tomato with the sesquiterpene biosynthetic pathway from a wild relative. *Proc. Natl. Acad. Sci. USA*, **109**, 20124–20129.

Breeden, D.C. and Coates, R.M. (1994) 7-Epizingiberene, a novel bisabolane sesquiterpene from wild tomato leaves. *Tetrahedron*, **50**, 11123–11132.

Breeden, D.C., Young, T.E., Coates, R.M. and Juvik, J.A. (1996) Identification and bioassay of kairomones for *Helicoverpa zea*. *J. Chem. Ecol.* **22**, 513–539.

Brückner, K., Bozic, D., Manzano, D., Papaefthimiou, D., Pateraki, I., Scheler, U., Ferrer, A., de Vos, R.C., Kanellis, A.K. and Tissier, A. (2014) Characterization of two genes for the biosynthesis of abietane-type diterpenes in rosemary (*Rosmarinus officinalis*) glandular trichomes. *Phytochemistry*, **101**, 52–64.

Brückner, K. and Tissier, A. (2013) High-level diterpene production by transient expression in Nicotiana benthamiana. *Plant Methods*, **9**, 46. https://doi.org/10.1186/1746-4811-9-46

Carter, C.D., Sacalis, J.N. and Gianfagna, T.J. (1989) Zingiberene and resistance to Colorado potato beetle in *Lycopersicon hirsutum* f. *hirsutum*. *J. Agric. Food Chem.* **37**, 206–210.

Choi, Y.E., Lim, S., Kim, H.J., Han, J.Y., Lee, M.H., Yang, Y., Kim, J.A. and Kim, Y.S. (2012) Tobacco NtLTP1, a glandular-specific lipid transfer protein, is required for lipid secretion from glandular trichomes. *Plant J.* **70**, 480–491.

Coates, R.M., Denissen, J.F., Juvik, J.A. and Babka, B.A. (1988) Identification of alpha-santalenoic and endo-beta-bergamotenoic acids as moth oviposition stimulants from wild tomato leaves. *J. Org. Chem.* **53**, 2186–2192.

Copati, M.G.F., Alves, F.M., Dariva, F.D., Pessoa, H.P., Dias, F.O., Carneiro, P.C.S., Carneiro, D.J.H. and Nick, C. (2019) Resistance of the wild tomato *Solanum habrochaites* to *Phytophthora infestans* is governed by a major gene and polygenes. *An. Acad. Bras. Cienc.* **91**, e20190149.

Dahan-Meir, T., Filler-Hayut, S., Melamed-Bessudo, C., Bocobza, S., Czosnek, H., Aharoni, A. and Levy, A.A. (2018) Efficient in planta gene targeting in tomato using geminiviral replicons and the CRISPR/Cas9 system. *Plant J.* **95**, 5–16.

Dawood, M.H. and Snyder, J.C. (2020) The alcohol and epoxy alcohol of zingiberene, produced in trichomes of wild tomato, are more repellent to spider mites than zingiberene. *Front. Plant Sci.*, **11**, 35.

de Azevedo, S.M., Faria, M.V., Maluf, W.R., de Oliveira, A.C.B. and de Freitas, J.A. (2003) Zingiberene-mediated resistance to the South American tomato pinworm derived from *Lycopersicon hirsutum* var. *hirsutum*. *Euphytica*, **134**, 347–351.

Engler, C., Kandzia, R. and Marillonnet, S. (2008) A one pot, one step, precision cloning method with high throughput capability. *PLoS One*, **3**, e3647.

Engler, C., Youles, M., Gruetzner, R., Ehnert, T.M., Werner, S., Jones, J.D., Patron, N.J. and Marillonnet, S. (2014) A Golden Gate modular cloning toolbox for plants. *ACS Synth. Biol.* **3**, 839–843.

Evidente, A., Cimmino, A. and Andolfi, A. (2013) The effect of stereochemistry on the biological activity of natural phytotoxins, fungicides, insecticides and herbicides. *Chirality*, **25**, 59–78.

Fan, P.X., Miller, A.M., Schilmiller, A.L., Liu, X.X., Ofner, I., Jones, A.D., Zamir, D. and Last, R.L. (2016) *In vitro* reconstruction and analysis of evolutionary variation of the tomato acylsucrose metabolic network. *Proc. Natl Acad. Sci. USA*, **113**, E239–E248.

Farrar, R.R. and Kennedy, G.G. (1987) 2-undecanone, a constituent of the glandular trichomes of *Lycopersicon hirsutum* f. *glabratum* – effects on *Heliothis zea* and *Manduca sexta* growth and survival. *Entomol. Exp. Appl.* **43**, 17–23.

Firdaus, S., van Heusden, A.W., Hidayati, N., Supena, E.D., Mumm, R., de Vos, R.C., Visser, R.G. and Vosman, B. (2013) Identification and QTL mapping of whitefly resistance components in *Solanum galapagense*. *Theor. Appl. Genet.* **126**, 1487–1501.

Freitas, J.A., Maluf, W.R., Cardoso, M.D., Gomes, L.A.A. and Bearzotti, E. (2002) Inheritance of foliar zingiberene contents and their relationship to trichome densities and whitefly resistance in tomatoes. *Euphytica*, **127**, 275–287.

Frelichowski, J.E. and Juvik, J.A. (2001) Sesquiterpene carboxylic acids from a wild tomato species affect larval feeding behavior and survival of *Helicoverpa zea* and *Spodoptera exigua* (Lepidoptera: Noctuidae). *J. Econ. Entomol.* **94**, 1249–1259.

Frelichowski, J.E. and Juvik, J.A. (2005) Inheritance of sesquiterpene carboxylic acid synthesis in crosses of *Lycopersicon hirsutum* with insect-susceptible tomatoes. *Plant Breed.* **124**, 277–281.

Fridman, E., Wang, J.H., Iijima, Y., Froehlich, J.E., Gang, D.R., Ohlrogge, J. and Pichersky, E. (2005) Metabolic, genomic, and biochemical analyses of glandular trichomes from the wild tomato species *Lycopersicon hirsutum* identify a key enzyme in the biosynthesis of methylketones. *Plant Cell*, **17**, 1252–1267.

Goffreda, J.C. and Mutschler, M.A. (1987) Potato aphid feeding response to *Lycopersicon pennellii* type-IV trichome exudate and trichome exudate components. *HortScience*, **22**, 1073.

Goffreda, J.C., Mutschler, M.A., Ave, D.A., Tingey, W.M. and Steffens, J.C. (1989) Aphid deterrence by glucose esters in glandular trichome exudate of the wild tomato, *Lycopersicon pennellii*. *J. Chem. Ecol.* **15**, 2135–2147.

Goncalves, L.D., Maluf, W.R., Cardoso, M.D., de Resende, J.T.V., de Castro, E.M., Santos, N.M., do Nascimento, I.R. and Faria, M.V. (2006) Relationship between zingiberene, foliar trichomes and repellence of tomato plant to *Tetranychus evansi*. *Pesqui. Agropecu. Bras.* **41**, 267–273.

Gonzales-Vigil, E., Hufnagel, D.E., Kim, J., Last, R.L. and Barry, C.S. (2012) Evolution of TPS20-related terpene synthases influences chemical diversity in the glandular trichomes of the wild tomato relative *Solanum habrochaites*. *Plant J.* **71**, 921–935.

Haggard, J.E., Johnson, E.B. and St Clair, D.A. (2013) Linkage relationships among multiple QTL for horticultural traits and late blight (*P. infestans*) resistance on chromosome 5 introgressed from wild tomato *Solanum habrochaites*. *G3*, **3**, 2131–2146.

Haggard, J.E., Johnson, E.B. and St Clair, D.A. (2014) Multiple QTL for horticultural traits and quantitative resistance to *Phytophthora infestans* linked on *Solanum habrochaites* chromosome 11. *G3*, **5**, 219–233.

Hawthorne, D.J., Shapiro, J.A., Tingey, W.M. and Mutschler, M.A. (1992) Trichome-borne and artificially applied acylsugars of wild tomato deter feeding and oviposition of the Leafminer *Liriomyza trifolii*. *Entomol. Exp. Appl.* **65**, 65–73.

Ishii, T., Matsuura, H., Kaya, K. and Vairappan, C.S. (2011) A new bisabolane-type sesquiterpenoid from *Curcuma domestica*. *Biochem. Syst. Ecol.* **39**, 864–867.

Johnson, E.B., Haggard, J.E. and St Clair, D.A. (2012) Fractionation, stability, and isolate-specificity of QTL for resistance to *Phytophthora infestans* in cultivated tomato (*Solanum lycopersicum*). *G3*, **2**, 1145–1159.

Jones, D.R. (2003) Plant viruses transmitted by whiteflies. *Eur. J. Plant Pathol.* **109**, 195–219.

Khrimian, A., Shirali, S. and Guzman, F. (2015) Absolute configurations of zingiberenols isolated from ginger (*Zingiber officinale*) rhizomes. *J. Nat. Prod.* **78**, 3071–3074.

King, R.R., Calhoun, L.A., Singh, R.P. and Boucher, A. (1990) Sucrose esters associated with glandular trichomes of wild *Lycopersicon* species. *Phytochemistry*, **29**, 2115–2118.

Leckie, B.M., De Jong, D.M. and Mutschler, M.A. (2012) Quantitative trait loci increasing acylsugars in tomato breeding lines and their impacts on silverleaf whiteflies. *Mol. Breed.* **30**, 1621–1634.

Leckie, B.M., De Jong, D.M. and Mutschler, M.A. (2013) Quantitative trait loci regulating sugar moiety of acylsugars in tomato. *Mol. Breed.* **31**, 957–970.

Leckie, B.M., Halitschke, R., De Jong, D.M., Smeda, J.R., Kessler, A. and Mutschler, M.A. (2014) Quantitative trait loci regulating the fatty acid profile of acylsugars in tomato. *Mol. Breed.* **34**, 1201–1213.

Lemke, C.A. and Mutschler, M.A. (1984) Inheritance of glandular trichomes in crosses between *Lycopersicon esculentum* and *Lycopersicon pennellii*. *J. Am. Soc. Hortic. Sci.* **109**, 592–596.

Lu, X., Zhang, L., Zhang, F., Jiang, W., Shen, Q., Zhang, L., Lv, Z., Wang, G. and Tang, K. (2013) AaORA, a trichome-specific AP2/ERF transcription factor of *Artemisia annua*, is a positive regulator in the artemisinin biosynthetic pathway and in disease resistance to *Botrytis cinerea*. *New Phytol.* **198**, 1191–1202.

Luckwill, L.C. (1943) *The Genus Lycopersicon*: a Historical, Biological, and Taxonomic Survey of the Wild and Cultivated Tomatoes. Aberdeen: Aberdeen University Press.

Maluf, W.R., Campos, G.A. and Cardoso, M.D. (2001) Relationships between trichome types and spider mite (*Tetranychus evansi*) repellence in tomatoes with respect to foliar zingiberene contents. *Euphytica*, **121**, 73–80.

Maluf, W.R., Silva, V.D., Cardoso, M.D., Gomes, L.A.A., Neto, A.C.G., Maciel, G.M. and Nizio, D.A.C. (2010) Resistance to the South American tomato pinworm *Tuta absoluta* in high acylsugar and/or high zingiberene tomato genotypes. *Euphytica*, **176**, 113–123.

Michels, K., Heinke, R., Schöne, P., Kuipers, O.P., Arnold, N. and Wessjohann, L.A. (2015) A fluorescence-based bioassay for antibacterials and its application in screening natural product extracts. *J. Antibiot.*, **68**, 734–740.

Mutschler, M.A., Doerge, R.W., Liu, S.C., Kuai, J.P., Liedl, B.E. and Shapiro, J.A. (1996) QTL analysis of pest resistance in the wild tomato *Lycopersicon pennellii*: QTLs controlling acylsugar level and composition. *Theor. Appl. Genet.* **92**, 709–718.

Nelson, D.R. (2009) The cytochrome p450 homepage. *Hum. Genomics*, **4**, 59–65.

Polavarapu, P.L. (2016) Determination of the absolute configurations of chiral drugs using chiroptical spectroscopy. *Molecules*, **21**(8), 1056.

Ralston, L., Kwon, S.T., Schoenbeck, M., Ralston, J., Schenk, D.J., Coates, R.M. and Chappell, J. (2001) Cloning, heterologous expression, and functional characterization of 5-epi-aristolochene-1,3-dihydroxylase from tobacco (*Nicotiana tabacum*). *Arch. Biochem. Biophys.* **393**, 222–235.

Sallaud, C., Rontein, D., Onillon, S. *et al.* (2009) A novel pathway for sesquiterpene biosynthesis from *Z,Z*-farnesyl pyrophosphate in the wild tomato *Solanum habrochaites*. *Plant Cell*, **21**, 301–317.

Scheler, U., Brandt, W., Porzel, A. *et al.* (2016) Elucidation of the biosynthesis of carnosic acid and its reconstitution in yeast. *Nat. Commun.* **7**, 12942.

Schilmiller, A.L., Charbonneau, A.L. and Last, R.L. (2012) Identification of a BAHD acetyltransferase that produces protective acyl sugars in tomato trichomes. *Proc. Natl Acad. Sci. USA*, **109**, 16377–16382.

Schilmiller, A.L., Moghe, G.D., Fan, P.X., Ghosh, B., Ning, J., Jones, A.D. and Last, R.L. (2015) Functionally divergent alleles and duplicated loci encoding an acyltransferase contribute to acylsugar metabolite diversity in *Solanum* trichomes. *Plant Cell*, **27**, 1002–1017.

Schilmiller, A.L., Schauvinhold, I., Larson, M., Xu, R., Charbonneau, A.L., Schmidt, A., Wilkerson, C., Last, R.L. and Pichersky, E. (2009) Monoterpenes in the glandular trichomes of tomato are synthesized from a neryl diphosphate precursor rather than geranyl diphosphate. *Proc. Natl Acad. Sci. USA*, **106**, 10865–10870.

Schuurink, R. and Tissier, A. (2020) Glandular trichomes: micro-organs with model status? *New Phytol.* **225**, 2251–2266.

Snyder, J.C., Guo, Z.H., Thacker, R., Goodman, J.P. and Stpyrek, J. (1993) 2,3-Dihydrofarnesoic acid, a unique terpene from trichomes of *Lycopersicon hirsutum*, repels spider-mites. *J. Chem. Ecol.* **19**, 2981–2997.

Sumner, L.W., Amberg, A., Barrett, D. *et al.* (2007) Proposed minimum reporting standards for chemical analysis Chemical Analysis Working Group (CAWG) Metabolomics Standards Initiative (MSI). *Metabolomics*, **3**, 211–221.

Takahashi, S., Yeo, Y.S., Zhao, Y., O'Maille, P.E., Greenhagen, B.T., Noel, J.P., Coates, R.M. and Chappell, J. (2007) Functional characterization of premnaspirodiene oxygenase, a cytochrome P450 catalyzing regio- and stereo-specific hydroxylations of diverse sesquiterpene substrates. *J. Biol. Chem.* **282**, 31744–31754.

Takahashi, S., Zhao, Y., O'Maille, P.E., Greenhagen, B.T., Noel, J.P., Coates, R.M. and Chappell, J. (2005) Kinetic and molecular analysis of 5-epiaristolochene 1,3-dihydroxylase, a cytochrome P450 enzyme catalyzing successive hydroxylations of sesquiterpenes. *J. Biol. Chem.* **280**, 3686–3696.

Tissier, A. (2012) Glandular trichomes: what comes after expressed sequence tags? *Plant J.* **70**, 51–68.

Tissier, A., Morgan, J.A. and Dudareva, N. (2017) Plant volatiles: going 'in' but not 'out' of trichome cavities. *Trends Plant Sci*, **22,** 930–938.

van der Hoeven, R.S., Monforte, A.J., Breeden, D., Tanksley, S.D. and Steffens, J.C. (2000) Genetic control and evolution of sesquiterpene biosynthesis in *Lycopersicon esculentum* and *L. hirsutum*. *Plant Cell*, **12**, 2283–2294.

Veening, J.W., Smits, W.K., Hamoen, L.W., Jongbloed, J.D. and Kuipers, O.P. (2004) Visualization of differential gene expression by improved cyan fluorescent protein and yellow fluorescent protein production in *Bacillus subtilis*. *Appl. Environ. Microbiol.* **70**, 6809–6815.

Vosman, B., Kashaninia, A., Van't Westende, W., Meijer-Dekens, F., van Eekelen, H., Visser, R.G.F., de Vos, R.C.H. and Voorrips, R.E. (2019) QTL mapping of insect resistance components of *Solanum galapagense*. *Theor. Appl. Genet.* **132**, 531–541.

Weber, E., Engler, C., Gruetzner, R., Werner, S. and Marillonnet, S. (2011) A modular cloning system for standardized assembly of multigene constructs. *PLoS One*, **6**, e16765.

Werner, S., Engler, C., Weber, E., Gruetzner, R. and Marillonnet, S. (2012) Fast track assembly of multigene constructs using Golden Gate cloning and the MoClo system. *Bioeng. Bugs*, **3**, 38–43.

Zabel, S. and Tissier, A. (2015) European patent application EP 3 178 313 A1: gene and protein for the synthesis of oxidized zingiberene derivatives. Applicant: Leibniz Institute of Plant Biochemistry. Filed on December 9th, 2015 and published on June 14th, 2017.